Comprehensive Final Report for CDFA Agreement Number 17-0514-000-SA: "GENOME EDITING OF *TAS4, MIR828* AND TARGETS *MYBA6/A7*: A CRITICAL TEST OF *XYLELLA FASTIDIOSA* INFECTION AND SPREADING MECHANISMS IN PIERCE'S DISEASE"

Principal Investigator (PI): Christopher D. Rock, Texas Tech University, Dept of Biological Sciences, mailstop 3131, Lubbock, TX 79409-3131. Ph (806) 834-4803. Email: chris.rock@ttu.edu
Cooperator: David Tricoli, University of California Davis Ralph Parsons Foundation Plant Transformation Facility.192 Robbins Hall, Davis, CA 95616. Phone (530) 752-3766. Email: dmtricoli@ucdavis.edu.

Time period covered by this report: January 1, 2018 - June 30, 2019.

INTRODUCTION

The Board suggested (RFP Dec. 2017, pp. A1-3) knocking out genes involved in diffusible signals and host chemical specificity for PD etiology by gene editing technology called CRISPR, and awarded an initial grant#15-0214SA to the PI. The short-term nature of funding cycles and attendant line-item reports can obscure the big picture-like why should CDFA support transgenic projects that take many years to develop? Our charge as researchers is to delivery practical and timely solutions to stakeholders. Yet we still do not know the underlying mechanisms of host resistance to PD, the roles nutrients play in disease states, the nature of pleiotropic PD symptoms like leaf scorch, shriveling berries, matchstick petioles, cane bark islands[1], or effects on root physiology (**Fig. 1**). If we design experiments to prove cause and effect (structural gene changes), we could gain insights into the mechanisms underlying the etiology of PD and leverage knowledge to develop cogent strategies to engineer host tolerance.

The threat of another PD epidemic like in southern California in the 1880s and again in 1990s remains real. Look to southern Italy where olive quick decline syndrome is decimating centuries-old olive groves[2] to appreciate the risk. As a translational researcher new to the field it is humbling to read Pierce's 1892 monograph[3]. Here quoted the first sentences which frame the issue faced yet today: "*The vine interests of California are of greater national than local importance. Locally nearly all horticultural interests are large, and the State, though deriving a liberal return from the grape, is not dependent upon it. On the other hand, the entire country is at present almost wholly dependent on California for domestic raisins and wines of the better class. The future will hardly change these relations…. Should some disease destroy the grape crop of California every State in the Union would be forced to send money to foreign countries for raisins and fine brands of wine... too much cannot be done to guard and stimulate the industry.*"

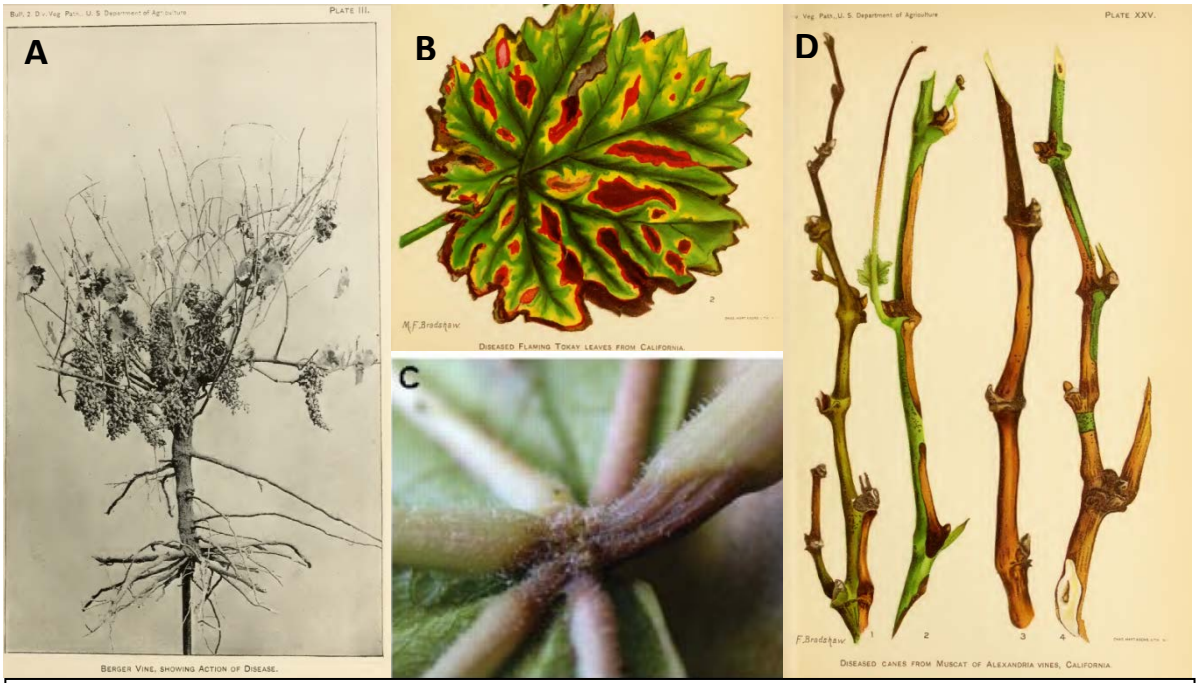

Fig. 1. Pleiotropic symptoms of Pierce's disease. A) whole plant. B) leaf scorch and rings of anthocyanin/chlorosis bordering healthy blade parenchyma. C) abscission of leaves at distal end, leading to 'matchstick petioles'. D) Green cane bark islands. Panels A,B,D: from Pierce [3]; Panel C from [1].

The xylem-limited bacterium *Xylella fastidiosa* (XF) is the causal agent of Pierce's disease (PD) in grapes and is a major threat to fruit, nut, olive, and coffee groves. PD is vectored by xylem sap-sucking insects and vector feeding preferences for XF-infected vines and olfactory cues like secondary metabolites of host plants may be important for PD etiology. Obvious PD symptoms are anthocyanin (red pigment) accumulation in leaves at the scorched periphery and shriveling of berries that impacts fruit quality and yield. The etiology of pleiotropic symptoms such as matchstick petioles and green cane islands by XF is not understood. Prior work demonstrated that XF infection causes a significant increase in calcium and decrease in leaf elemental phosphorus (P) content of leaves[4], but the bioavailable form of P and the molecular mechanisms underlying these phenomena are unknown. Our working hypothesis (**Fig. 2**) is that inorganic phosphate (P_i)- and sugar-regulated[5] microRNAs (miRNAs), initially described in Arabidopsis[6] and associated with host P_i derangement in citrus greening disease Huanglongbing (HLB)[7], mediate pleiotropic PD symptoms by deranging host Post-Transcriptional Gene Silencing mechanisms including amplification by miR828-triggered production of phased small-interfering RNAs (phasi-RNAs) targeting *MYBA5/6/7* transcription factors that control anthocyanin biosynthesis[8, 9]. We have been successful at making inroads into understanding molecular mechanisms and have submitted the work to date for review by *The Plant Cell* and *Transgenic Research* journals. We have also filed an invention disclosure to our institution on enablement via genome editing technology of a pending patent application that claims *MIR828, TAS4*, and *MYB* targets. Recently the USDA issued a directive that the agency does not have plans to regulate plants generated using gene editing techniques that create deletions/insertions that could otherwise have been developed through traditional breeding techniques and are not developed using plant pests as donor (except complete null segregants which are exempt, like those produced by outcrossing/breeding). This development provides a path for commercialization of value-added genome-edited grapevine without expensive regulatory proscriptions.

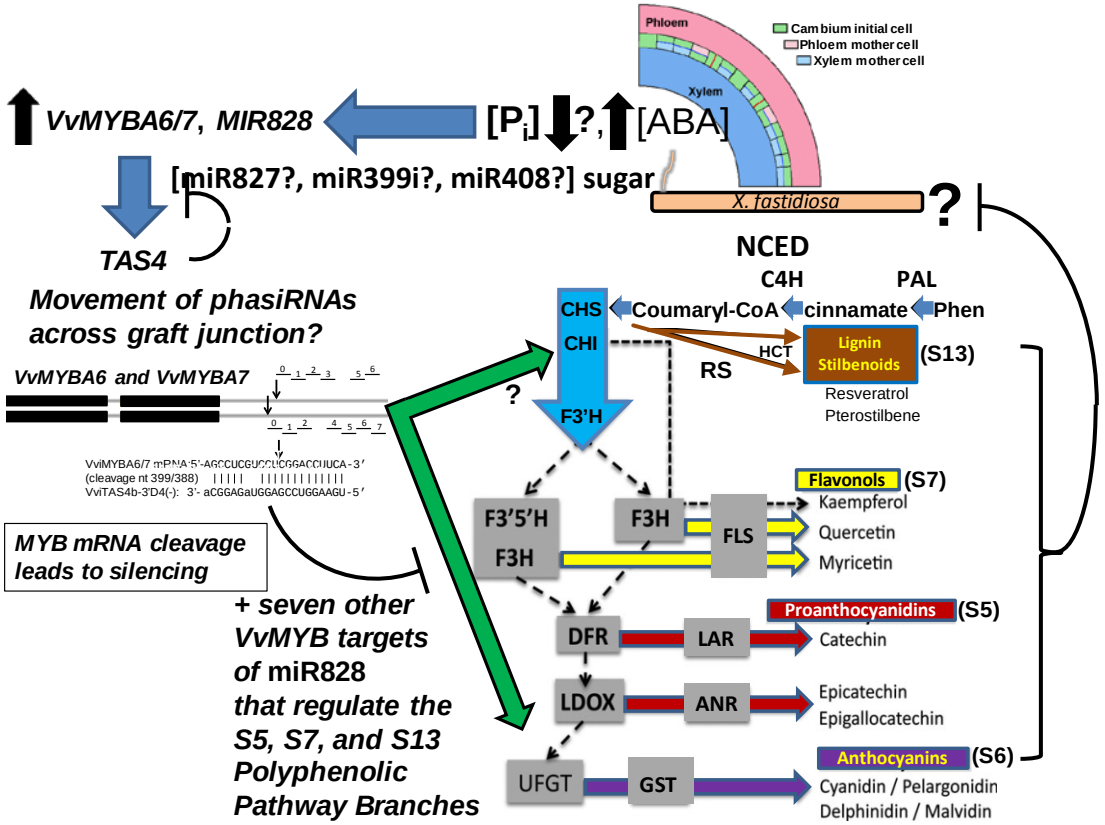

Fig. 2. Initial model of how XF symptoms are manifested through hypothesized decreases in host xylem phosphate and/or elevated ABA during infection, leading to induction of VvMYBA6/7 which along with miR828 effect *TAS4* and homologous MYBs expression. *TAS4* and miR828 antagonize expression of target MYBs controlling multiple polyphenolic biosynthetic branch pathways that evidence suggests antagonize XF growth. If *MIR828* is knocked out, the prediction is that loss of *TAS4* function to normally silence *VvMYBA6/7* could improve XF resistance and conversely, if *VvMYBA6/7* is knocked out, XF virulence could increase. See [5, 8].

OBJECTIVES OF PROPOSED RESEARCH AND PATH TO APPLICATION:

I. Test the miR828, *TAS4*, and target *MYBA6/7* functions in PD etiology and XF infection and spreading by genome editing using CRISPR/Cas9 transgenic technology.

II. Characterize tissue-specific expression patterns of *TAS4*, *MIR828* primary transcripts, sRNAs, and *MYB* and other miRNA target genes in response to XF infections in the field and in edited genotypes.

III. Characterize the changes in control versus edited genotypes for (a) xylem sap [P_i], and (b) polyphenolic levels of XF-infected canes and leaves. If results are conclusive based on greenhouse studies, in the future we will conduct field trials and collaborate to carry out insect diet preference/behavioral modification/fitness assays on defended transgenic materials. (c) Test the P_i analogue Phi as a durable, affordable and environmentally sound protectant/safener for PD.

DESCRIPTION OF ACTIVITIES CONDUCTED TO ACCOMPLISH OBJECTIVES

I. Test the miR828, *TAS4*, and target *MYBA6/7* functions in PD etiology and XF infection and spreading by genome editing using CRISPR/Cas9 transgenic technology.

We used *Agrobacterium* strain EHA105 carrying binary p201N-gRNA-cas9 vectors[10] targeting the *MIR828*, *TAS4ab*, and *MYBA6* and *MYBA7* loci (**Fig. 3a**) to transform embryogenic callus derived from anthers of the commercially relevant grapevine rootstock 101-14[11] which produces requisite marker anthocyanins for phenotyping of events. Grape transformation with p201N-gRNA-cas9 yielded two kanamycin resistant *TAS4b* plants (*TAS4b1, TAS4b2*), six *MYBA6* plants (*MYBA6* -1, -2, -3, 4, -6 and -7) and six *MYBA7* plants (*MYBA7* -1, -2, -3, 5, -6 and -8). We also obtained two empty vector (with no gRNA cassette) transgenic plants (cas9-1, cas9-2). T-DNA integration of kanamycin-resistant plants was characterized by Southern blotting with the *nptII* probe and *cas9* probe. Digestion of DNA with *Hind*III and hybridization with the *nptII* probe is predicted to yield junction fragments longer than 4.3 kb. The integration of *cas9* was confirmed by digestion of genomic DNA with *Bam*HI enzyme. Junction fragments longer than 2.7 kb are expected to hybridize. Southern blot analysis showed that all of the transgenic plants had one to several integrated copies of the T-DNA with the *nptII* gene (**Fig. 3b**) and *cas9* probes (**Fig. 3c**). Junction fragment analysis revealed that MYBA7-2 and -3 were plants that regenerated from the same transformation event (**Fig. 3b, c**).

To identify candidate genome-edited events in transgenic plants, polyacrylamide gel electrophoresis-based genotyping[12] was performed. PAGE heteroduplex analysis is based on the rationale that DNA heteroduplexes migrate at a slower rate than homoduplexes in polyacrylamide gels. PCR amplification of target sequences results in mixture of amplicons including the edited allele. Denaturation and renaturation of PCR products result in homoduplexes and heteroduplexes with different migration rate. Based on the difference in migration of bands, **Figure 4A** shows evidence for one candidate editing event for *TAS4b*, and at least two editing events for *MYBA7*.

A 300 bp gRNA target region was PCR amplified from each transgenic line and vector-alone control with partial Illumina adapter sequences incorporated in the 5' end of the primers. The PCR product was gel-purified and subjected to Amplicon-EZ target amplicon sequencing (Genewiz, South Plainfield, NJ) (**Fig. 4B**). The in-frame three bp deletions for characterized MYBA7 lines #5 and #6 are predicted to delete residue 8^{Arg} from the polypeptide, whereas the biallelic A/G single bp insertion dual mutations in lines 1-3 and 8 are predicted to cause translation termination after residue 13^{Asp}. We also observed a single bp insertion in TAS4b line #1 and 3 bp deletion in TAS4b #2.[13]

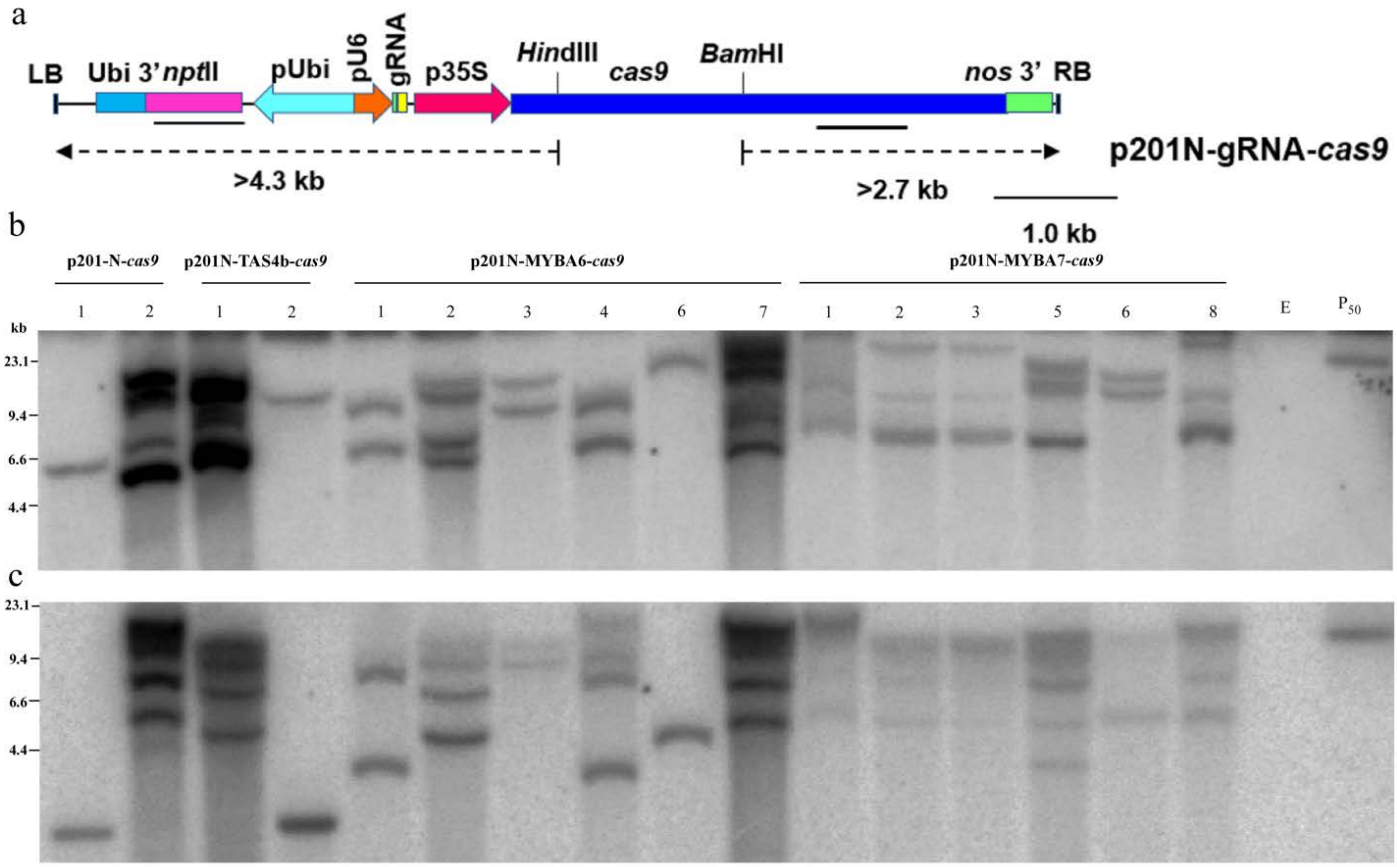

Fig. 3. Analysis of grape plants transformed with p201N-gRNA-cas9. **a)** The T-DNA of the binary vector p201N-gRNA-*cas9*. p201N-gRNA-*cas9* harbors gRNA in p201N-*cas9*. RB: T-DNA border-right, p35S: Cauliflower mosaic virus (CaMV) 35S promoter, *cas9*: CRISPR associated protein 9 human-codon optimized, *nos 3'*: polyadenylation signal of the nopaline synthase gene, pU6: *Medicago truncatula* U6.6 promoter, gRNA: guide RNA, pUbi: ubiquitin promoter, *npt*II: neomycin phosphotransferase gene, Ubi 3': Ubiquitin polyadenylation signal, LB: T-DNA border-left. Probes used (*npt*II and *cas9*) have been marked in bold lines. The junction fragment sizes >4.3 kb and >2.7 kb has been marked in a dashed arrow. **b)** and **c)** Southern blot analysis of grape plants transformed with p201N-gRNA-*cas9* using *npt*II probe and *cas9* probe, respectively. Total DNA was extracted from 16 transformed plants (two p201N-*cas9*, two p201N-TAS4b-*cas9*, six p201N-MYBA6-*cas9* and six p201N-MYBA7-*cas9*) that regenerated and rooted under kanamycin selection **b)** DNA (10 µg) was digested with *Hin*dIII and probed with *npt*II coding sequence. Junction fragments of >4.3 kb from transgenic plants are expected to hybridize. The binary plasmid p201N-MYBA6-*cas9* digested with *Hin*dIII (P_{50}) was used as a positive control c**)** DNA (10 µg) was digested with *Bam*HI and probed with *cas9* coding sequence. Junction fragments of >2.7 kb from transgenic plants are expected to hybridize. The binary plasmid p201N-MYBA6-*cas9* digested with *Bam*HI (P_{50}) was used as a positive control.

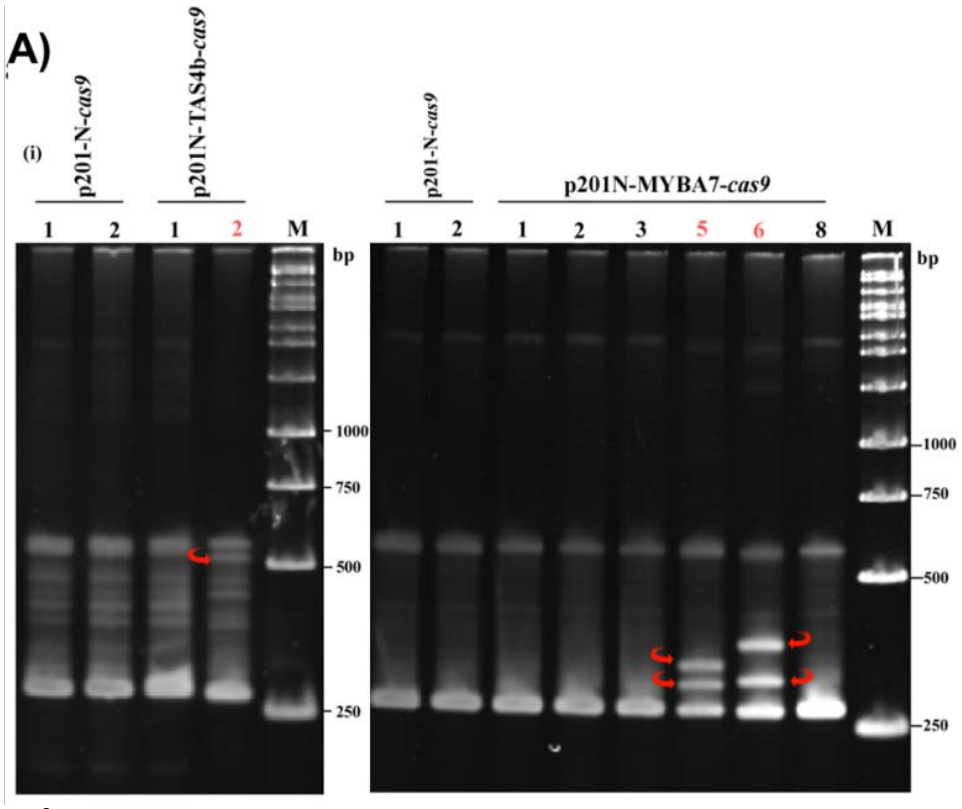

B)

Target Sequence	TAS4b-3'D4(-)		Number reads/total (%)		Event#
TAS4b-rc	5'-..TGATTGGTGGCCATGGTGAAGGT_CCGAGGTAGAGGCACCTTA..-3'	WT	233039/238683	(97.6)	
m#1	5'-..TGATTGGTGGCCATGGTGAA---_CCGAGGTAGAGGCACCTTA..-3'	(-3)	12/9613	(0.1)	1
m#2	5'-..TGATTGGTGGCCATGGTGAAGGTTCCGAGGTAGAGGCACCTTA..-3'	(+1)	6559/9613	(68.2)	1
m#3	5' ..TCATTCGTCGCCCATCGCTGAACGTTCCCAGGTACAGCCACCTTA.. 3'	(+1)	14/3780	(0.4)	2
m#4	5'-..TGATTGGTGGCCATGGTGAA---_CCGAGGTAGAGGCACCTTA..-3'	(-3)	3160/3780	83.6)	2

AA:	M E G S L G L R K G A W T S				
MYBA7startcodon	5'-..ATGGAGGGCTCTTTAGGTCTGCG_GAAAGGTGCTTGGACTAGTG..-3'	WT	69562/71044	(97.9)	
m#1	5'-..ATGGAGGGCTCTTTAGGTCTGCGAGAAAGGTGCTTGGACTAGTG..-3'	(+1)	1189/4415	(26.9)	1
m#2	5'-..ATGGAGGGCTCTTTAGGTCTGCGGGAAAGGTGCTTGGACTAGTG..-3'	(+1)	2311/4415	(52.3)	1
m#3	5'-..ATGGAGGGCTCTTTAGGTCTGCGAGAAAGGTGCTTGGACTAGTG..-3'	(+1)	138/560	(24.6)	2
m#4	5'-..ATGGAGGGCTCTTTAGGTCTGCGGGAAAGGTGCTTGGACTAGTG..-3'	(+1)	418/560	(74.6)	2
m#5	5'-..ATGGAGGGCTCTTTAGGTCTGCGAGAAAGGTGCTTGGACTAGTG..-3'	(+1)	37/111	(33.3)	3
m#6	5'-..ATGGAGGGCTCTTTAGGTCTGCGGGAAAGGTGCTTGGACTAGTG..-3'	(+1)	71/111	(64.0)	3
m#7	5'-..ATGGAGGGCTCTTTAGGTCTGCGAGAAAGGTGCTTGGACTAGTG..-3'	(+1)	8/21	(38.1)	5
m#8	5'-..ATGGAGGGCTCTTTAGGTCT---_GAAAGGTGCTTGGACTAGTG..-3'	(-3)	13/21	(61.9)	5
m#9	5'-..ATGGAGGGCTCTTTAGGTCTGCGAGAAAGGTGCTTGGACTAGTG..-3'	(+1)	5/10	(50.0)	6
m#10	5'-..ATGGAGGGCTCTTTAGGTCT---_GAAAGGTGCTTGGACTAGTG..-3'	(-3)	5/10	(50.0)	6
m#11	5'-..ATGGAGGGCTCTTTAGGTCTGCGAGAAAGGTGCTTGGACTAGTG..-3'	(+1)	7/22	(31.8)	8
m#12	5'-..ATGGAGGGCTCTTTAGGTCTGCGGGAAAGGTGCTTGGACTAGTG..-3'	(+1)	13/22	(59.1)	8

Fig. 4. Evidences for genome editing of *TAS4b* and *MYBA7* in transgenic grapevine events produced to date. **A)** Polyacrylamide gel electrophoresis heteroduplex amplicon assay [12] showing candidate editing events in stably transformed grapevine regenerants (red arrows). p201-N-cas9: empty vector control regenerants. **B)** Validation by deep sequencing of amplicons for independent grapevine *TAS4b* and *MYBA7* CRISPR editing events (far right column) resulting in 1 nt insertions (yellow) and 3 nt deletions (dashes) at expected positions 3 nt upstream of the Proximal Adjacent Motif (PAM; blue) in target guide sequences (red). The *MYBA7* insertion events result in a stop codon five amino acids downstream from frame shifts. High confidence events are boxed (blue) based on high percentages of reads abundance, which varied for different amplicons (e.g. MYBA7#6) due to technical variations from fee-for-service provider, despite evidence for editing, panel A.

Many labs have demonstrated high efficiency (~80% including biallelic/homozygous mutations in primary transformants) of plant genome editing by CRISPR/Cas9 synthetic guide technologies (reviewed in[14, 15]). Recent results show the method is practical for engineering resistance in grapefruit to citrus canker[16] caused by the bacterium *Xanthomonas axonopodis* by modifying the PthA4 pathogenicity effector binding elements in the promoter of *Cs-Lateral Organ Boundaries1* susceptibility gene. Three recent reports documented the efficacy of events by CRISPR/Cas9 *Agrobacterium*-mediated transformation/regeneration in grapevine: targeting *Vv-Phytoene Desaturase* in cv Muscat as visible marker for bi-allele knockout efficiency[17], the *Vv-WRKY52* gene (~70% biallelic events) in cv Thompson seedless for resistance to noble rot caused by *Botrytis cinerea*[18], and the *Vv-L-idonate dehydrogenase/IdnDH* gene for tartaric acid biosynthesis in cv Chardonnay[19]. In each case, and especially the latter a preponderance of events were one bp insertions and three bp deletions, like we observe for predominantly bi-allelic *Vv-TAS4b* and *Vv-MYBA7* regenerants (**Fig. 4B**). Proposed future experiments will employ multiple guide constructs[13] to target all *MYBA* and *TAS4* family members, and to target the sole *Vv-MIR828* locus at locations upstream or downstream of the mature miR828 in the hairpin structure to generate leaky dominant-negative alleles predicted to alter DICER processing efficiency. Our initial test construct for *Vv-MIR828* aimed to create null alleles by targeting the mature miR828 duplex *per se*, but we failed to recover any regenerants, consistent with a speculated essential function of *MIR828*.

We have propagated these events by rooting cuttings from the primary transformants. We have now six vector alone control plants growing in the greenhouse, five TAS4b-m plants, 17 MYB6-m plants, and 15 MYBA7-m plants.

Target specificity is an important issue for all genome editing technologies, including CRISPR/Cas. Off-targets have been addressed with experimental evidence for some off-target activity in rice but not in *N. benthamiana* (reviewed in [15]). Cas9 activity is not affected by DNA methylation- an affirmation of the power of the technique in eukaryotes. Off-target mutations are less problematic because they can easily be outcrossed (including the effector construct T-DNA), and the chances minimized by computational target design (http://crispr.hzau.edu.cn/CRISPR2/). We have proposed to assess vector feeding preferences[20] on our genome-edited anthocyanin host effector lines. Host species switches induced by XF inter-sub-specific homologous recombination is a potential concern[21] regarding the ability of XF to adapt to engineered genotypes. Strong selection pressures on XF due to new technologies may eventually lead to new pathogen variants capable of breaking down resistance. Thus, management practices to combine all possible prophylactic and modes of resistance/tolerance should be developed in parallel with genome editing to prolong use of all resistance technologies being developed.

Summary of Objective I accomplishments: We characterized and propagated several independent transgenic events constituting single base insertions and trinucleotide deletions of the miR828-triggered *TAS4b* and *MYBA7* target genes generated by Clustered Regularly Interspaced Short Palindromic Repeats genome editing technology (CRIPSR/Cas9). This technology can result in non-"genetically modified organism" (GMO) grapevines and rootstocks after outcrossing the effector transgene locus. Our results enable advances to understand the molecular mechanisms underlying PD host-pathogen interactions, disease dynamics, and pleiotropic PD symptoms. Dissolution of the chimeric state of mutated and non-mutated cells to obtain homozygous plants for desired mutations by back-crossing and genetic segregation is a lengthy route for grapevine because of the difficulty of successful crosses with greenhouse material, and several years of time elapsed before regenerated juvenile transgenics can flower. We have proposed to continue the work which will include field plantings under a USDA-BRS permit to conduct crosses.

II. Characterize tissue-specific expression patterns of *TAS4, MIR828* primary transcripts, sRNAs, and *MYB* and other miRNA target genes in response to XF infections in the field and in edited genotypes.

a. Studies on transgenic tobacco overexpressing anthocyanin effector AtMYB90

Uninfected and XF-infected non-transgenic control, *AtMYB90*-hemizygous and homozygous plant leaf samples from 2016 greenhouse XF challenge experiments were used for systems analysis of differential expression of mRNAs by RNA-seq. The RNA-seq reads were mapped to the tobacco draft reference transcriptome by kallisto[22]. The experimental design made to interrogate the genotype effect (the effect of overexpressing transgene *AtMYB90*) and the infection effect (infected vs non-transgenic control) is as described in **Table I**. When log2-fold-change (LFC) of > |2|, and multiple-testing Bonferroni-Hochberg adjusted $p < 0.05$ for statistical significance was used as the cut-off for differential expression, XF-infection resulted in an overall reduction in differentially expressed genes when compared

to the expression changes caused by genotype (**Table I**). **Figure 5** depicts the metabolic overview of significant differentially expressed pathway genes under different experiment conditions listed in **Table I**. In addition to the *AtMYB90*/*PAP2* transgene over-expression, gene families involved in secondary metabolism such as Phenylalanine ammonia-lyase, Chalcone--flavonone isomerase, Chalcone synthase, Chalcone isomerase, Anthocyanidin reductase-binding domain, Anthocyanidin 3-O-glucosyltransferase, and Anthocyanidin synthase were the top up-regulated genes when the genotype effect was considered in homozygous and heterozygous plants (**Fig. 5A, C**; data not shown). Interestingly, all the above genes were down-regulated when the infection effect was considered (**Fig. 5B, D**). Downregulation of phosphate transporter and several nitrate transporter genes upon infection was observed as over-represented in metabolic overview (**Fig. 5B, E**; data not shown). Abolishment of nitrate transporter NRT2.1 gene function in Arabidopsis results in a quick and stronger response against ascomycetes such as *Plectosphaerella cucumerina*[23] and reduced susceptibility to *Pseudomonas syringae* by salicylic acid priming and interfering with pathogen effectors[24].

Table I. Schematic of various tobacco RNA-seq comparisons described in Results and the number of significantly differentially expressed genes

	Genotype effect		**Infection effect**			
	Homozygous plants vs control plants*	**Hemizygous plants vs control plants***	**Homozygous infected vs control uninfected#**	**Hemizygous infected vs control uninfected#**	**Control infected vs control uninfected#**	**All infected vs All uninfected***
Upregulated LogFC >2	282	211	123	63	6	67
Downregulated - LogFC <2	81	83	118	50	8	50
Total	363	294	241	113	14	117

*padj value

pvalue

We analyzed the sRNA datasets from the 2015-2016 tobacco XF-challenge experiments with the statistical software DESeq2[25] for computational identification of differentially expressed clusters of small RNA-producing loci, focusing on *MIRNA*s. We previously presented in July 2017 progress report Principal Component Analysis evidence that replicate experiments gave concordant results. The experimental design to decipher the genotype effect (the effect of overexpressing transgene *AtMYB90*) and the infection effect (infected vs non-transgenic control) on sRNAs is as described in **Table I** for RNA-seq data. The canonical sliced targets (174 cases) for the differentially expressed miRNAs were identified using CleaveLand (data not shown). Although not statistically significant, miR828a and *TAS4*ab were down-regulated by overall XF challenge, confirming results from sRNA blots presented in the July 2016 progress report. Interestingly, upregulation of miR828 (not statistically significant) and TAS4ab was observed when the genotype effect and infection effect of homozygous and hemizygous plants were considered. This further substantiates the conservation of the autoregulatory involving nta-miR828/NtTAS4ab/AN2 loop in tobacco. TAS4-3'D4(-) self-targets the *TAS4a* and *-b* transcripts, but degradome analysis did not reveal AtMYB90 to be a perfect target to tobacco TAS4 3'(D4-) (data not shown). In addition, miR398, miR399, miR168, and miR166 were significantly down regulated by XF infection. Inorganic phosphate transporter; *PHT1;7*, the target of miR399, was also found to be downregulated significantly upon infection. miR397 was downregulated (not significantly) while its target LACCASE family members showed significant upregulation (data not shown). Inverse correlation was observed between miR168 abundance and that of its target ARGONAUTE1 (albeit not significantly). Downregulation of miR398 has been shown in Arabidopsis plants challenged with avirulent strains of *Pseudomonas syringae* that causes bacterial speck[26]. Interestingly, miR827, miR159/319, miR156, miR390, and miR167 were up-regulated

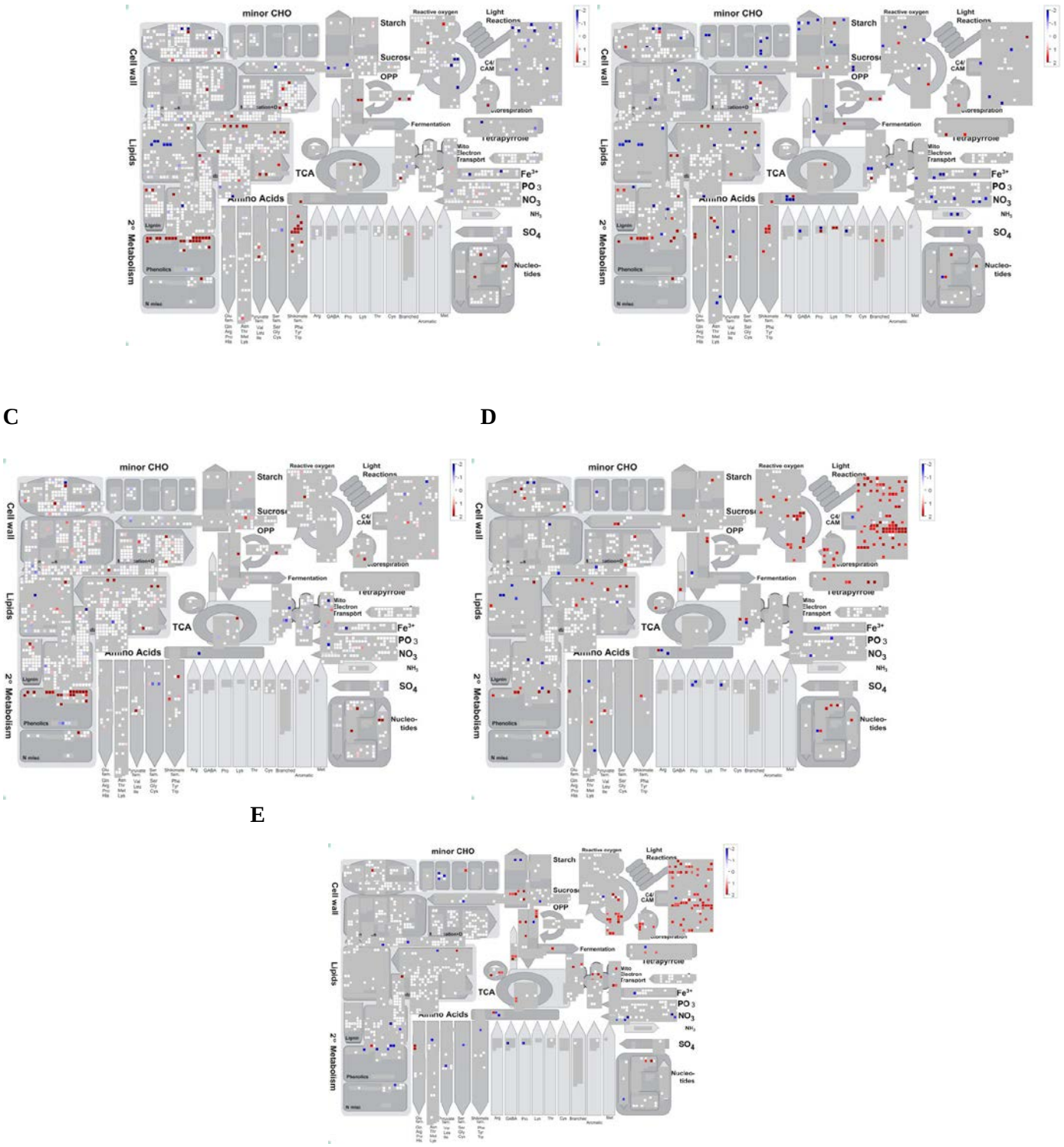

Fig. 5. Metabolic overview (Mapman) of significantly differentially expressed genes in transgenic tobacco XF-challenged plants measured by RNA-Seq. Red indicates up-regulated by XF infection, blue indicates down regulation. A) Homozygous plants vs control plants B) Homozygous infected vs control uninfected C) Hemizygous plants vs control plants D) Hemizygous infected vs control uninfected E) control infected vs control uninfected**.**

upon XF-infection, consistent with the working hypothesis and results (see below) of grapevine PD symptomatic and control sRNA libraries. Significant up regulation of miR159/miR319, miR156 correlated with down regulation (albeit not significantly) of their target transcription factors TCP, MYB and Squamosa Promoter Binding proteins. The most interesting result was the XF down regulation of tobacco homolog of sly-miR10539 upon XF-infection and concordant upregulation of its target polyphenol oxidase, an anthocyanin oxidizing enzyme (data not shown).

b. 1. Studies on grapevine miRNAs and their targets

Table II lists the cumulative grapevine sRNA and RNA-Seq library quality control parameters through data pre-processing to remove ribosomal RNAs, t-RNAs, and snoRNAs[27] and genome[28] annotation stages of samples characterized to date. The statistical power from multiple replicates across years will drive defensible claims at the publication stage, which has been completed for the multiple biological replicates for three years, 2015- 2017.

Table II. Quality control parameters* of sequenced sRNA libraries from 2015-2017 Temecula PD-infected samples.

sRNA libraries. Sample/Year	raw reads (million)	%rRNA, tRNA	%snoRNA	trimmed, clean reads (million)	%MIRNAs$
Leaf, PD2015	7.83	66.29	5.76	3.22	13.30
Leaf, Con2015	2.91	65.27	6.18	1.22	34.49
Leaf, PD2016.1	16.13	81.76	4.41	4.67	29.62
Leaf, PD2016.2	54.08	82.46	4.21	15.56	39.44
Leaf, Con2016.1	5.16	48.08	6.05	2.39	47.89
Leaf, Con2016.2	8.70	46.20	5.64	4.39	35.11
Leaf,PD2017.1	4.54	85.29	2.59	0.53	18.49
Leaf,PD2017.2	10.97	69.26	3.63	3.05	22.18
Leaf, Con2017.1	37.55	65.59	5.64	15.45	14.80
Leaf, Con2017.2	16.38	56.41	3.65	7.83	21.03
Petiole,PD2017	15.51	45.52	4.60	8.34	17.25
Petiole,Con2017	10.31	81.72	5.81	3.45	6.15
RNA-seq transcriptome libraries. Sample/Year†					
Leaf, PD2016.1	38.67	1.10	0.33	38.24	trace
Leaf, PD2016.2	33.96	0.69	0.15	33.73	trace
Leaf, Con2016.1	39.52	0.79	0.06	39.21	trace
Leaf, Con2016.2	26.07	11.28	0.08	23.13	trace
Leaf, PD2017.1	17.68	3.14	0.01	17.46	trace
Leaf, PD2017.2	45.12	7.39	0.04	37.63	trace
Leaf, Con2017.1	29.42	1.23	0.01	28.49	trace
Leaf, Con2017.2	24.91	16.56	0.07	23.06	trace
Petiole, PD2017	36.30	0.07	0.03	36.26	trace
Petiole, Con2017	37.30	0.58	0.02	37.07	0.01

*datasets mapped to *Vitis vinifera* 12X genome sequence, version NCBI RefSeq GCF_000003745.3 [28] with bowtie [77] after trimming adapter with fastx-toolkit (http://hannonlab.cshl.edu/fastx_toolkit/).
$ mapped to miRBase22 plant MIRNA hairpins (http://www.mirbase.org/)
† mapped to ref transcriptome with kallisto-sleuth [30].

A fourth set of PD-infected and candidate control samples (> four biological replicates) was collected from the 'Calle Contento' vineyard in Temecula CA on July 23-25, 2018. **Table III** shows results of anthocyanin quantitations for these samples, which have significantly higher anthocyanin concentrations than healthy controls sampled from the same vineyard. Select samples were prepared into libraries and sequenced by the Institute for

Integrative Genome Biology (IIGB) at UC Riverside and are currently being analyzed for inclusion at the publication stage, if warranted based on results in addition to the three consecutive sample year results in hand.

Table III. Anthocyanin quantitation of XF-infected candidate Merlot leaves from 'Calle Contento' vineyard, Temecula CA, July 2018

Condition	µmoles cyanidin-O-glucoside equiv/mg fresh weight	s.e.m.	pval*
control healthy	8.5	0.9	
PD symptoms	22.7	3.3	0.02

* significantly different than control, two-sided Student's t-test, unequal variance assumed (n=4)

We collected PD symptomatic samples from the same Temecula CA vineyard over three years which allowed for high-confidence systems analysis of differential expression of miRNAs, phasiRNAs and mRNAs by RNA-Seq. **Figure 6** shows principal component analysis (PCA) of the differences in PD field samples versus controls across three years for 200,000 phasiRNA loci and 219 *MIRNA* loci called de novo by ShortStack and validated for all annotations in miRBase22[29]. The good clustering of PD versus controls for dimensions of treatment and replicates across years that encompass >60% of all variation demonstrates a robust experimental design for statistical inference.

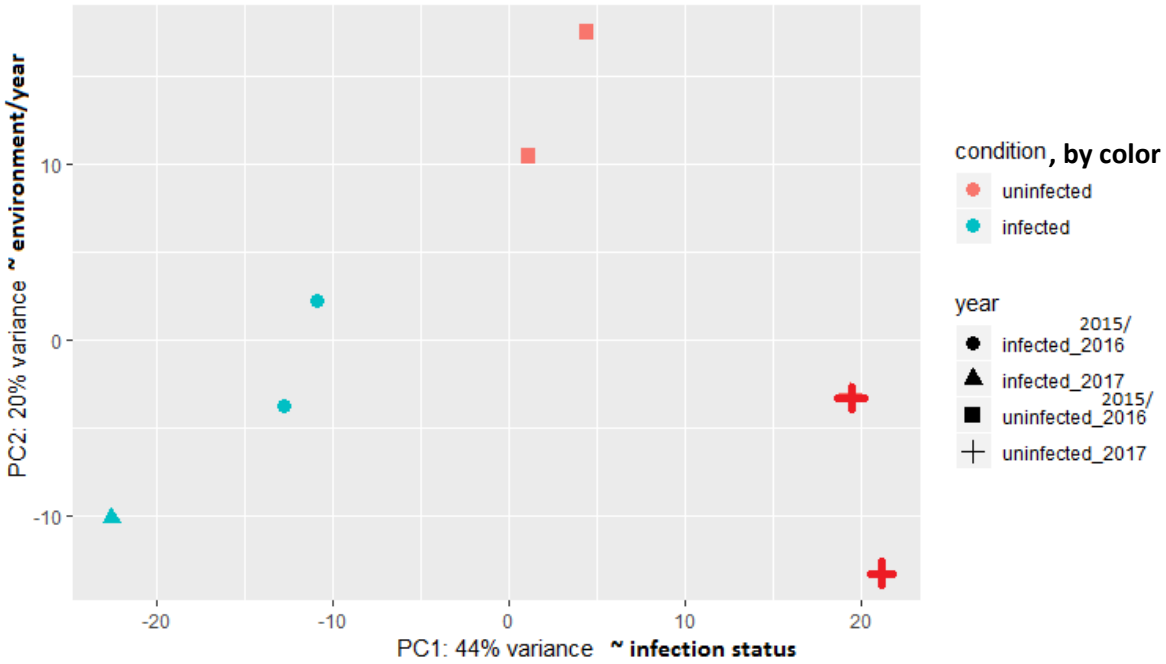

Fig. 6. Principal component (PC) analysis of seven grape leaf libraries from Temecula CA field samples representing sRNA-generating loci subjected to differential expression analysis. The percentage of variation is depicted in the PC1 and PC2 axes. Based on clustering of samples, PC1 represents the major dimension of Pierce's disease symptoms that was the basis for sample collection and PC2 is inferred to capture the environmental variation across years.

RNA-Seq data was mapped to the reference transcriptome with kallisto/sleuth[30]. We obtained 1,329 differentially expressed genes (793 up, 536 down) with expression above a threshold (>30 reads mapped to a transcript per library on average), a log2-fold-change (LFC) of > |2|, and multiple-testing Bonferroni-Hochberg adjusted $p < 0.05$ for statistical significance. This is comparable to the 1,240 (977 up, 263 down) DE genes for a similar greenhouse XF challenge experiment recently published by the Dandekar group[31]. For the 13 genes claimed differentially regulated by XF infection and quantification validated by RT-PCR (in Figs. 3 and 6B of Dandekar's *FPS* paper)[31], we observe a

good concordance with our results (correlation coefficient= 0.75, $p < 0.05$), however only eight of our results are statistically significant, suggesting differences exist between the published greenhouse results and our field and/or leaf samples, read depths of libraries (see Table II), and/or methods (**Table IV**). **Table V** compares our MapMan[32] RNAseq Gene Ontology classification results of 1,240 top XF DE genes with the top 1,240 DE genes reported by the Dandekar group for greenhouse XF challenge RNAseq[31].

Table IV. Comparison between recently reported DE of 14 genes in XF-challenged greenhouse leaves versus our RNAseq DE calculations on four Temecula CA field sample biological replicates harvested in 2016/17. Significant LFC values in **bold.** Note the sole discordant result for Fold Change sign (line in *italics*) is for a very low-expressed gene and is therefore discounted.

Annotation	**GeneID**	**Dandekar LFC**	**our LFC***	**Mean expressed**	**our padj**
PR-2/beta1,3-glucanase	VIT_06s0061g00100	6.64	6.43	4659	**2.75E-21**
PR-1	VIT_03s0088g00810	5.32	2.03	635	1.27E-01
PR-8; chitinase	VIT_05s0094g00200	1.58	2.30	21	**4.68E-02**
HSP18	VIT_08s0058g00210	4.32	4.21	6	**2.60E-04**
HSP17	VIT_04s0008g01520	3.58	4.97	50	**5.51E-14**
HSP4	VIT_07s0031g00670	2.32	1.90	303	**9.23E-04**
Nucleoredoxin-1	VIT_01s0127g00520	2.81	1.58	91	**3.23E-02**
Peroxidase	*VIT_00s1677g00010*	*1.14*	*-0.10*	*4*	*9.58E-01*
ferritin5	VIT_13s0067g01840	-1.00	-0.58	1066	4.17E-01
Sucrose synthase	VIT_07s0005g00750	3.46	1.62	7345	**4.40E-02**
Pectin lyase	VIT_14s0066g01060	1.72	0.23	24	8.25E-01
UDP-glycosyltransferase	VIT_17s0000g04750	1.07	0.37	857	6.13E-01
Xyloglucan-endotransglucosylase	VIT_06s0061g00550	2.32	4.71	174	**4.31E-04**
thaumatin-like protein	VIT_18s0001g14480	2.00	0.76	589	6.58E-01
	Pearson of LFCs, R=	0.75		**Binomial p-val†**	**0.05**

* kallisto-sleuth method [30].
† bionomial distribution probability of 13 successful LFC values being the right sign in 13 tests when DE up regulated =79% probability (true for 12 of 13 genes; a conservative estimate) based on results reported in [31].

Table V. Comparison of Gene Ontology over-represented terms metrics of project field sample PD RNAseq versus published greenhouse XF challenge RNAseq results [31]

MapMan Gene Ontology term	MapMan fold over-represented field RNAseq	Field expt MapMan pval	Greenhouse RNAseq PANTHER Gene Ontology term	Greenhouse PANTHER fold enrichment	Greenhouse expt PATHER pval
phenylpropanoid metabolism	576	0.00001	phenylpropanoid metabolic process	5.85	0.0012
flavonoid metabolism	2610	0.049	flavonoid biosynthetic process	5.23	0.0016
TCA/organic acid transformation	6.3	0.002	carboxylic acid transport	4.95	0.016
cell wall	124	0.15	cell wall organization or biogenesis	2.68	0.0035
glycolysis	5.4	0.002	carbohydrate catabolic process	3.56	0.034
UDP glucosyl and glucoronyl transferase	28	0.014	UDP-glucosyltransferase activity	4.73	0.037
transport -p and v-ATPase H+ exporting ATPase	20	0.009	transmembrane transporter activity	2.16	0.008

Figure 7 shows a systems biology Metabolic Overview of gene ontology[32] for mRNAs significantly differentially expressed by XF infections in the field, highlighting the lignin, phosphate regulation, and polyphenolics/anthocyanin pathways known as subject to canonical miRNA slicing activities[9]. The top ontology bin overrepresented for DE expression was secondary metabolism: phenolics and flavonoids (Benjamini-Hochberg adjusted $P < 1E^{-20}$). These results are highly concordant with recently published mRNA-Seq results for grapevine XF challenge experiments in the greenhouse[31] that we analyzed in the 2018 Proceedings report; of the 594 significantly differentially expressed genes for the greenhouse experiment which were also significantly differentially expressed (padj < 0.05) in our field sample libraries, only 16 (< 3%) had a relative sign change for up/down effects and the majority of these cases were expressed at low levels in our samples (i.e., likely 'shot noise' effects[33]). The Pearson correlation coefficient for LFC magnitudes of our results for these genes versus those reported[31] was 0.80, demonstrating the reproducible effects of XF infections on gene expression across greenhouse and field environments, like we described previously for tobacco greenhouse and field grapevine *TAS4* and miR828.

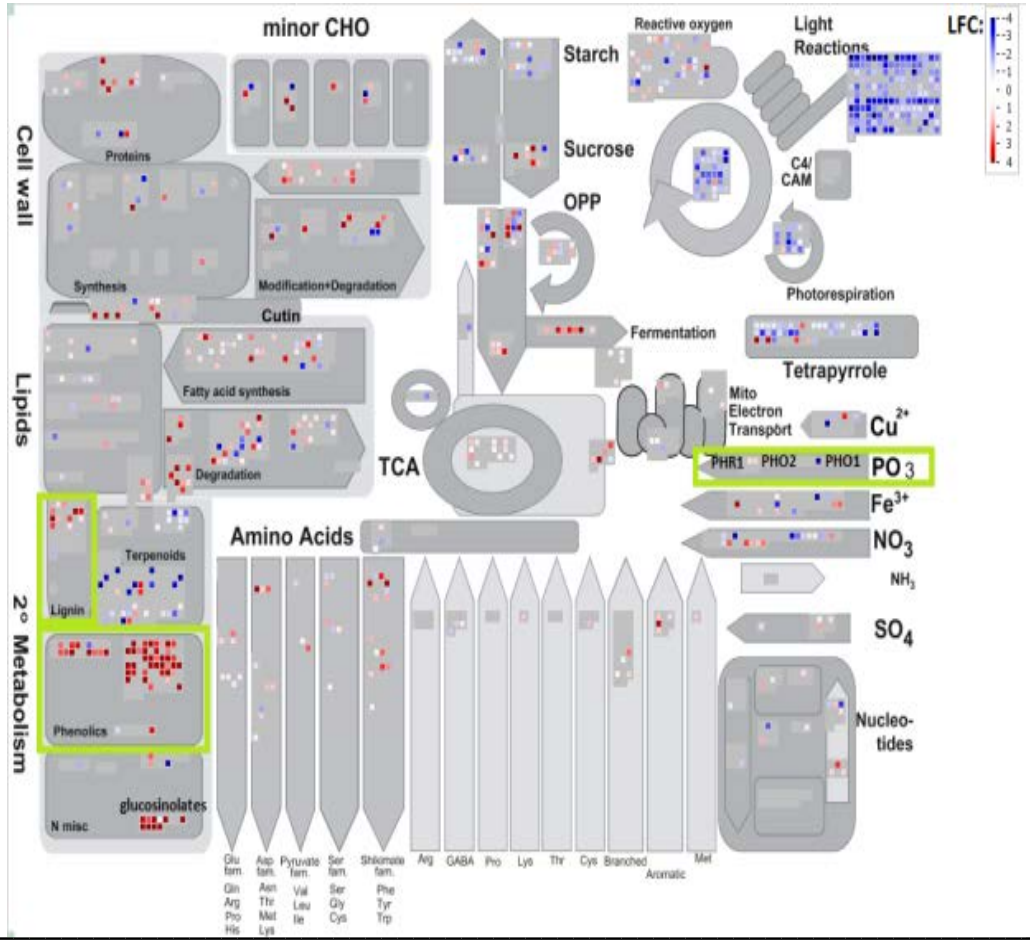

Fig. 7. Metabolic overview (Mapman) [32] of significantly differentially expressed genes measured by RNA-Seq from three years (2015-2017) of PD field samples from Temecula CA. Red indicates up-regulated by XF infection, blue indicates down regulation. Overexpression of pathways (boxed green) regulated by miR828/*TAS4* (phenolics), miR399/827 (phosphate effectors PHR1, PHO2, PHO1, PHT5), and miR397/408 (lignin) **support** the working model that XF infection results in changes of mRNAs via hypothesized miRNA derangements. Our results are strongly concordant with recently published [31] transcriptome changes in greenhouse experiments that reported the response circuitry of winegrape to XF infection.

Table VI lists the significantly differentially expressed[33] *MIRNA* loci found in PD symptomatic field grapevine sample libraries. For each DE miRNA, the differential expressions quantified by mRNA-Seq[30] in the same samples for degradome-validated canonical target genes are also shown. We observed only significant down-regulations of miRNA expressions in PD symptomatic field samples. This observation is similar to a recent report for copper-regulated miRNAs (associated with oxidative stress responses) in grapevine[34]. Several miRNA target mRNA loci with differentially expressed mRNAs, but that do not produce phasiRNAs and few siRNAs, are evidenced by sRNA reads below the expression cutoff and/or a lack of Dicer size call by ShortStack. There was a good correlation between the direction of differential mRNA expression in PD symptomatic leaves and concordant direction of siRNA abundance changes, for examples miR408 target *VIT_15s0021g01390*/*Phytocyanin* (but not *VIT_06s0004g07420*/*laccase13* which has some phasiRNA production; **Table VI**), miR397 target laccases, and miR156/319/396/398/399 targets. This expected null observation supports the hypothesis that opposite sign changes between phasiRNAs and source template mRNAs is indicative of slicing/silencing activities by phasiRNAs. Of particular interest in this regard based on association with regulatory networks controlling fruit development[35, 36], abiotic[9]-, and biotic-stress[7] responses were miR858 and *TAS4*/miR828/*MYB* phasiRNA-producing target genes that encompass orthologues of *MYB-L3* triggered by miR828 in many species[35-43] including grape[44]. Also fitting the inverse pattern for down-regulated miRNAs and phasiRNAs and some up-regulated miRNA target mRNAs were phosphate-regulated miR391/399/827/408 described in other species[6, 45] targeting, respectively, phasiRNA-producing

Ca^{2+}-translocating ATPase10/ACA10[46] associated with anthocyanin biosynthesis[9, 47], *MAJOR FACILITATOR SUPERFAMILY (MFS)* RING-finger ubiquitin E3 ligases, *PHO2* E2 conjugase, and/or phosphate translocators[45, 48, 49] for miR399/827, and Cu homeostasis proteins involved in P_i- and osmotic stress responses, pollen tube growth, insect feeding resistance, and photosynthesis[50-54] for miR408. miR408 is down-regulated in Arabidopsis as a late (14 hr) response to bacterial pathogen *Pseudomonas syringae* whereas its target *Plantacyanin* mRNA increases[55], similar to our finding (**Table VI**).

Inverse correlations were observed between XF significantly down-regulated miRNAs and concordant up-regulated targets: in particular miR858-like/828 and *MYB-PAL3/AtMYB4-like*, miR408 and a *Phytocyanin*, *TAS4b* and *MYBA6*, miR391/3627-like and *ACA10*, miR397a and *Laccase7/11-like*, miR394bc and *F-box X6*, several miR399 family members and predicted targets *PHT1;7* and novel *BULB lectin-like*, miR398abc and *Blue Copper-Binding Protein*, miR319bcf and plant-specific transcription factor *TEOSINTE BRANCHED/CYCLOIDEA/PCF TCP24-like* and a novel *CCHC Zinc Finger*, and miR396bg-like and *GROWTH REGULATING FACTOR/GRF9* (**Table II**). *MIR827-like* was nearly significantly down regulated ($P = 0.06$) however the predicted canonical targets *PHO1;H3* and *MFS/SUGAR TRANSPORTER6/STP6* were not validated by degradome analysis nor were they differentially expressed in our PD field sample libraries. However, nearly half (21) of all 47 expressed MFS nitrate transporters based on Gene Ontology were significantly differentially regulated in PD symptomatic field samples, which MapMan[32] analysis quantified as significantly over-represented for the process 'carrier-mediated solute transport' ($P < 0.04$, Benjamini-Hochberg multiple tests corrected). This observation suggests that complex cross-regulation between nitrate and phosphate transporter families may be important in XF host responses, as has been documented for *PHT* transporter family members *per se* in response to phytoplasma effectors[56] and inorganic ion deficiencies[57]. For example, *VvPHT5/NITROGEN LIMITATION ADAPTATION-like* gene *VIT_07s0005g00280*, an unlikely target of miR399, was significantly up-regulated (LFC=2.18, $P_{adj} < 0.0005$, as were two homologues of MYB TF *PHOSPHATE STARVATION RESPONSE1 (PHR1*; *VIT_07s0005g04120* LFC=0.53, P_{adj}=0.07; *VIT_14s0036g01380* LFC=1.11, P_{adj}= 0.0007). PHR1 is required for phytoplasma effector SAP11-triggered P_i starvation responses in Arabidopsis[56]. Two studies previously documented mis-regulation of phosphate transporter *VvPHT2;1* and *MFS/SPX1* in response to 8 weeks XF incubation in grapevine[58] and at 9 days post-XF infection in Arabidopsis[59].

Table VI. DESeq2 imputed differential expression of miRNAs and target mRNAs by XF infection for anthocyanin pathway protein-coding genes and phosphate-regulated miRNAs supports miRNAs as effectors of PD symptoms of anthocyanin accumulation (MYBs), 'green islands' (lignin), and 'matchstick petioles' (auxin/Ca^{2+} signaling). Empirical data-driven expression results from 3 years of field samples and degradome validation of slicing activities. Up-regulated phasiRNAs are in **bold**.

***MIRNA* Locus Annotation**/validated targets	**siRNA baseMean expression**	**LogFold Change**	***P* value**	**PhaseScore, 21nt; SSclass**	**RNAseq LFC**	**RNAseq adj.pval**
Phe-Ammonia Lyase VIT_06s0004g02620	49.9	**4.22**	7.8E-05	N.A.†	3.43	4.5E-05
Raffinose synthase VIT_11s0016g05770	757	**5.99**	5.0E-09	N.A.†	4.29	1.3E-09
Anthocyanidin synthase VIT_02s0025g04720	254	**6.73**	7.3E-10	N.A.†	5.74	3.4E-12
Chalcone synthase3 VIT_05s0136g00260, *CHS3*	204	**5.32**	1.3E-07	N.A.†	6.25	8.5E-12
***Xylella fastidiosa* genome sRNAs**	2766	**3.67**	4.4E-04	N.A.†	n.d.	n.d.
ath-miR858-like, Cluster_5544	452	-3.92	8.7E-04	N5		
vvi-miR858, Cluster_439214	11.6	-3.57	0.02	14.6;N11		
MYB-PAL3 VIT_09s0002g01380, target of both	64	-1.07	0.40	1478.0	2.19	0.027
VIT_04s0008g01800, novel AtMYB4-L	N.A.	N.A.	N.A.	N.A.†	2.87	3.2E-04
VIT_11s0016g01300, novel MYB/TT2-L	37.4	-0.61	0.52	97.7	1.14	0.17
VIT_09s0002g01400, MYB7_1[9]	N.A.	N.A.	N.A.	0.9	1.16	0.44
VIT_16s0050g00070, novel AtMYB17-L	N.A.	N.A.	N.A.	N.A.†	0.43	0.78
VIT_04s0008g01820, novel MYB/TT2-L	N.A.	N.A.	N.A.	0.4	-2.62	0.09
VIT_04s0008g01810, novel AtMYB4-L	N.A.	N.A.	N.A.	2.2	-2.19	0.16
VIT_07s0005g01210,MYBF1/MYB12-2[9]	N.A.	N.A.	N.A.	N.A.†	-1.41	0.30
VIT_05s0049g02260, novel AtMYB71-L	N.A.	N.A.	N.A.	N.A.†	-1.09	0.48

VIT_12s0059g00700, novel AtMYB101-L	1.5	-1.05	0.52	N.A.†	-0.12	1
vvi-miR408-3p, Cluster_164591	118	-2.5	0.003	817.9; N5		
VIT_15s0021g01390, Phytocyanin	5.9	**4.39**	0.002	N.A.†	6.74	8.5E-013
VIT_12s0034g01140, Phytocyanin	N.A.	N.A.	N.A.	N.A.†	0.59	0.74
VIT_06s0004g07420, laccase13*	1.5	-0.76	0.64	0.3	-0.21	0.61
***TAS4b,* Cluster_374453**	6,526	-3.2	0.006	16,011		
***TAS4a,* Cluster_374531**	24,646	-0.72	0.46	29,108	-0.24	1
***TAS4c,* Cluster_3762**	239	**1.28**§	0§	4060.5		
vvi-miR828/828*, Cluster_434978	1.3[#]	-1.83	0.31	16.6; N14		
MYBA6 VIT_14s0006g01290, D4(-)[9]	6.8	-3.81	0.02	68.7	0.57	0.76
MYBA5 VIT_14s0006g01340, D4(-)[9]	1.3	-1.85	0.29	23.1	0.15	1
MYBA7 VIT_14s0006g01280, target D4(-)[9]	0.03	0.03	0.98	87	-0.1	1
VIT_17s0000g08480, MYB157[9]	141	-1.88	0.13	2616	-2.65	0.09
VIT_14s0066g01220, MYB156not miR858targ[9]	43	-3.29	0.01	4416.8	-1.39	0.28
VIT_11s0016g01320, MYB PA2[9]	3.8	-3.12	0.06	12.1	-0.51	0.75
VIT_11s0016g05660, MYB 82B[9]^	N.A.	N.A.	N.A.	8.5	-0.51	1
VIT_04s0008g01870, MYB PAL2[9]^	4.1	-3.00	0§	13.9	-0.24	1
VIT_00s0341g00050, MYB PAL1[9]**^**	46.7	-1.75	0.14	1940	-0.1	0.86
VIT_08s0007g04830, MYB27[9]	N.A.	N.A.	N.A.	N.A.†	-0.11	1
VIT_01s0127g00730, MYB155[9]	9.6	-1.61	0.31	813	N.A.	N.A.
vvi-miR391-5p/3627-like, Cluster_138240	93	-2.85	0.007	599.7;Y	-1.35	1
miR5225-like, Cluster_443450	2	-0.73	0.63	Y		
vvi-miR3627-5p, 5' isomiR; Cluster_382347	84	0.29	0.78	122; N6		
VIT_11s0052g00320, *Ca^{2+}-ATPase10*	11.3	-2.04	0.07	171.7	0.37	0.37
vvi-miR397a-3p, Cluster_567895	32	-3.56	0.007	828.7;Y		
vca-miR397-like, Cluster_320031	1	**2.28**	0.21	N5		
VIT_08s0007g01550, LAC7-L*	N.A.	N.A.	N.A.	0.2	4.5	5.0E-05
VIT_08s0007g06460, LAC11-L	94	**1.46**	0.09	N.A.†	0.80	0.41
VIT_13s0019g01930, LAC17	1.0	**2.28**	0.21	1.1	0.42	1
vvi-miR394c-5p, Cluster_461976	22	-3.63	0.01	189.6;N14		
vvi-miR394b, Cluster_459260	1.2	-1.8	0.31	Y		
VIT_01s0010g03730, F-Box X6	7.6	**0.58**	0.64	N.A.†	0.90	0.11
vvi-miR399i, Cluster_32743	118	-3.35	0.015	307.3;Y		
vvi-miR399a, Cluster_243872	28	-2.71	0§	Y		
vvi-miR399b, Cluster_427860	2.3	-2.51	0.15	Y		
miR399-like, Cluster_243856	4.4	-1.96	0.22	Y		
VIT_07s0005g03300, PHT1;7*	1.9	-2.28	0.19	2.7	0.79	0.52
VIT_13s0067g03280, PHT1;3/PHO84*	1.6	-0.72	0.67	N.A.†	0.65	1
VIT_18s0166g00230, BULB lectin-like*	N.A.	N.A.	N.A.	N.A.†	1.53	0.006
VIT_18s0166g00250, Pro-rich extensin	13.7	**5.16**	5.8E-05	N.A.†	4.48	3.0E-39
VIT_18s0166g00260, membr-helical extensin	N.A.	N.A.	N.A.	N.A.†	2.19	0.03
vvi-miR3631b-3p, Cluster_111014	10.4	-2.65	0.018	15.5;N5		
VIT_00s1405g00010, Mediator SU16	n.d.	n.d.	n.d.	n.d.	-0.31	0.67
vvi-miR398a, Cluster_895	109	-2.41	0.02	Y		
vvi-miR398b, Cluster_152505	19	-1.1	0.37	N6		
vvi-miR398c, Cluster_151483	142	-1.06	0.32	N6		
VIT_11s0016g05530, blue copper-binding	31	**1.92**	0.09	N.A.†	2.37	0.01
VIT_09s0002g06000, Cyt-c oxidase Vb	0.8	**0.58**	0.74	N.A.†	0.22	0.65
VIT_14s0030g00830, Cu/Zn SOD CSD1	1.3	**0.70**	0.67	N.A.†	0.05	0.96
VIT_11s0016g05520, Plastocyanin-like	146	**3.23**	0§	N.A.†	-0.63	0.28
vvi-miR319c, Cluster_28674	32	-2.3	0.03	650.2;Y		
vvi-miR319b, Cluster_5298	8	-2.21	0.06	Y		

vvi-miR319f, Cluster_144125	5	-2.68	0.036	Y		
VIT_01s0011g02770, novel ZnFinger	1.5	**2.04**	0§	N.A.	0.75	0.02
VIT_10s0003g03910, TCP24-like	2.4	**0.85**	0.62	N.A.†	0.62	0.02
VIT_19s0014g01680, TCP4-like	21.3	**0.44**	0.67	N.A.†	-0.09	0.91
novel miR3629a-3p-like; Cluster_76173	6.3	-3.02	0.035	37.7;Y		
vvi-miR3629a-3p, Cluster_337960	18	-2.65	0.15	N14		
vvi-miR3629c-3p, Cluster_437137	0.8	-1.29	0.48	N14		
VIT_04s0008g05650, novel V-SNARE coil	6.5	**2.56**	0.08	N.A.†	0.52	0.48
ptc-miR396g-5p-like, Cluster_2543	392	-2.02	0.04	N5		
vvi-miR396b-5p, Cluster_269469	601	-1.67	0.09	N5		
vvi-miR396a, Cluster_220964	6.5	-1.57	0.19	Y		
VIT_15s0048g01740, GRF9	N.A.	N.A.	N.A.	2.6	1.54	0.007
VIT_02s0012g02250, VvbZIP05	5.0	**1.37**	0.38	N.A.†	0.16	0.61
VIT_02s0025g04910, GRF3	N.A.	N.A.	N.A.	1.7	-3.32	0.02
VIT_18s0001g08650, GRF1-like	N.A.	N.A.	N.A.	0.1	-2.57	0.004
VIT_16s0039g01450, GRF5	N.A.	N.A.	N.A.	0	-2.64	0.06
miR827-3p-like, Cluster_132568	853	-1.8	0.057	547.6;Y		
VIT_14s0108g01130, AtPHO1;H3/SPX*	N.A.	N.A.	N.A.	N.A.†	-0.31	0.80
VIT_13s0019g01330, AtSTP6/MFS*	n.d.	n.d.	n.d.	n.d.	-0.06	1
vvi-miR156d, Cluster_272101	92	-1.74	0.08	N5		
vvi-miR156c, Cluster_75786	23	-1.42	0.26	Y		
vvi-miR156f, Cluster_380020	226	-1	0.33	Y		
vvi-miR156g, Cluster_439950	236	-0.85	0.40	N5		
vvi-miR156i, Cluster_372522	17	-0.61	0.63	Y		
hvu-miR156b-like, Cluster_437250	0.5	-0.98	0.59	N11		
vvi-miR156h, Cluster_291677	0.7	-0.8	0.66	N5		
VIT_01s0010g03910, SPL13B	N.A.	N.A.	N.A.	N.A.	2.28	0.01
VIT_17s0000g05020, SPL6/LIGULELESS	1.1	**1.32**	0.43	N.A.†	1.19	0.09
VIT_12s0028g03350, SPL4_2	0.7	-0.80	0.66	0.1	-3.09	1.6E-05
VIT_10s0003g00050, SPL3	1.2	**0.55**	0.74	0.1	-1.32	0.03
VIT_01s0010g03710, SPL2_1	2.8	-0.46	0.77	N.A.†	-1.27	0.005
VIT_11s0065g00170, SPL2_3	1.9	-1.79	0.31	2.8	-0.71	0.02
vvi-miR395g, Cluster_8062	49	-2.19	0.09	848.6;Y		
vvi-miR395f, Cluster_8072	1.8	-2.29	0.15	Y		
vvi-miR395d, Cluster_8097	2.9	-2.24	0.17	Y		
vvi-miR395a, Cluster_8113	1.3	-1.32	0.45	Y		
VIT_05s0020g04210, APS1	10.5	**1.18**	0.27	N.A.†	0.52	0.25
VIT_18s0001g04890, AST68	2.2	-2.49	0.14	5.8	-1.49	0.11
DCL2; VIT_04s0023g00920, PHASI locus[9]	44	**0.46**	0.62	101.8	-0.81	0.06
SGS3; VIT_07s0130g00190, PHASI locus[9]	160	-1.59	0.10	628.4	-0.54	0.34
AGO2; VIT_10s0042g01150, PHASI locus	9.9	**0.77**	0.52	28.8	-0.45	0.46
AGO2-Like; VIT_10s0042g01180, PHASI locus	5.5	**0.86**	0.50	9.5	-0.23	0.82

† N.A.: These clusters of sRNAs were not called by ShortStack as having a dominant DICER activity size class. phasiRNA analyses for genes use the most abundant cluster mapping within genomic coordinates; if the cluster total reads abundance for all test libraries was below 37, no DE stats were calculated.

§ not determined by DESeq2 due to independent filtering of assumed outlier, defined by Cook's distance. LFC calculated manually. n.d.: not determined due to incompatible gramene.org mapping coordinates.

Star species quantification; mature species active based on degradome, but below sRNAseq detection limit [9].

* predicted target based on GSTAr; no degradome evidence.

^ modest degradome evidence for miR858-slicing 33 nt upstream from miR828 slice, reminiscent of reports for apple and peach [35, 36].

b. 2. Studies on PHAS loci associated with PD-symptomatic grapevine leaves

PHAS loci produce 21/22 nt phasiRNAs from DNA DEPENDENT RNA POLYMERASE II (Pol II)-generated transcripts triggered by action of miRNAs[60, 61] specifically 22 nt in length (called the '22_1' mechanism) or by the action of 21 nt miRNAs in association with AGO7 on two nearby adjacent targets in the mRNA, called the 'two-hit trigger,' or '21_2' mechanism described for miR390/*TAS3/ARF3/4*[62, 63] and miR156/172[39]. However in the case of 21 nt TAS4abc-3'D4(-) tasiRNAs found in numerous eudicots and identified in **Table VI** as differentially regulated in PD-symptomatic grapevine, it triggers phasiRNA production from target MYBs by an unknown 21_1 trigger mechanism[64]. We explored the PHAS space in grapevine with PhaseTank[65] to identify genes other than miR828/*TAS4* and miR391/*ACA10* (both '22_1' cases) possibly impacted by XF infection. We found over 230 PHAS loci and obtained evidence from independent degradome libraries[44, 66] for miRNA triggers of novel *TAS* loci in addition those conserved *TAS/PHAS* genes described previously[9]. **Table VII** lists select cases of PHAS loci whose 21 nt phasiRNAs were differentially expressed in PD-symptomatic grapevine leaves, and their degradome-validated trigger miRNA expressions. Of particular note is many of top-listed significantly differentially regulated *PHAS* and *TAS* genes were triggered by miR482 (which is down-regulated in PD-symptomatic leaves albeit not significantly) that cascades directly and via TAS-generated tasiRNAs both to and from the large Leucine-Rich-Repeat/LRR receptor family members[9, 67]. mRNA-Seq evidence indicated that over 150 LRRs out of the 341 such genes annotated in grapevine[68] were differentially regulated by XF infection in our datasets. Two loci *VIT_13s0047g00100/TAS11* and *VIT_18s0072g01090*/vvi-sly-TAS5-Like are annotated as 87/83aa peptides (probably not translated) and the derived sly-TAS5L phasiRNA 3'D12(-) targets NB-ARC LRR *VIT_00s0238g00130* and other LRRs[9]. The miR482-triggered phasiRNAs mostly decreased in PD-symptomatic leaves while several of the cognate target mRNAs in the cascades increased inversely in libraries made from the same samples (**Table VII**).

Table VII. PHAS/TAS loci and regulatory cascade targets other than miR828/*TAS4/MYB* and miR391/*ACA10* with significantly differentially expressed phasiRNAs or mRNA targets in PD-symptomatic leaves. Up-regulated in **bold**

Short Stack Cluster/PT PHAS#	Annotation	SS Phase Score	Phasi LFC	Phasi Pval	mRNA LFC	mRNA Padj	miRNA/ TAS trigger	miR/ TASI Allen score	Degrad Class	Slicing Pval[a-d]
103575/33	VIT_05s0077g00540	5829	-3.14	0.01	-1.00	0.54	miR390	4.5	2	0.02[b]
163788/185	*TAS3-like* chr7:4363868-4364133	292.5	-2.36	0.13	N.A.	N.A.	miR390 "21_2"	3	2	0.17[d]
294371/24	VIT_12s0059g0141062aa peptide *TAS3-like*[9] chr12: 6340329-6340741	4586	-2.89	0.013	-0.30	N.A.	miR390	2.0	0 4 2	0.001[b] 0.05[a] 0.13[d]
138128	ARF4/VIT_06s0004g03130, target of TAS3-3'D8(+)	27.1	-3.32	0.04	-2.61	4E-7	TAS3-5'D8(+)	0.5	3 2	0.015[b] 0.07[a]
242337	ARF3/VIT_10s0003g00420	22.5	-2.19	0.11	-1.02	0.01	TAS3-5'D8(+)		n.d.	
248453	ARF4-L/ VIT_10s0003g04100	2.3	-2.88	0.09	-2.40	4E-06	TAS3-5'D8(+)		n.d.	
288895	ARF4-L2/ VIT_12s0028g01170	55.5	**0.39**	0.77	-0.70	0.02	TAS3-5'D8(+)		n.d.	
161320/9	VIT_07s0104g01320 TIR1-like F box[9]	7026	-0.77	0.42	-0.99	0.08	miR393 "22_1"	4	2 0 2	0.005[a] 0.0004[b] 0.05[d]
378353/78	VIT_14s0068g01330 TIR1 F box[9]	1798	-0.34	0.68	**0.43**	0.40	miR393 (goes down XF, p~0.2)	1	2 0 2 2	0.005[a] .0004[b] 0.009[c] 0.05[d]
121163/162	VIT_05s0029g00390 H-loop-H[9]	479	-0.18	0.89	**0.79**	0.14	miR393	5	2	0.18[d]

355803/40	VIT_14s0030g01240 TIR1-like F-box[9]	1702	-0.18	0.86	**0.94**	0.18	miR393 TIR1L-3'D9(-) Self slicing	1 0	3 0 2 2 2 2 3 3	0.02[a] .0008[b] 0.02[c] 0.09[d] 0.04[a] 0.015[b] 0.004[c] 0.03[d]
334518/6&47	VIT_13s0047g00100 87aa peptide TAS11[9]	4107	-1.96	0.05	**0.43**	0.31	aqc-miR482c csi-miR482-like	3.5 5.5	4 0 2 2	0.03[a] 0.002[b] 0.04[c] 0.21[d]
481574/20	VIT_18s0072g01090 vvi-sly-TAS5L 83aa peptide; D6(+) slices LRRs on chr12 and D12(-) slices PHAS58:VIT_00s0238g00130[9]	4116	-0.54	0.54	**1.92**	0.04	miR482 miR3633a-cluster; goes down XF	2	2 2 2 2	0.01[a] 0.006[b] 0.02[c] 0.09[d]
224668/19	Intergenic TAS chr9:10397078-10397511	5525	-0.56	0.52	N.A.		unknwn	N.A.		
215637/82	VIT_09s0002g03330 RPS5-like	1418	-1.43	0.14	-2.00	0.001	PHASI1 9D2(+)	2.5	2 4 2 2	0.01[a] 0.02[b] 0.02[c] 0.09[d]
216440/86	VIT_09s0002g03980 RPS5-like	535	-2.04	0.04	-0.50	0.20	PHASI1 9D2(+)	4.5	2	0.17[d]
228287/105	VIT_09s0070g00350 AAA+_ATPase	190	-0.22	0.83	-1.64	0.02	PHASI1 9D2(+)	3.5	2	0.25[d]
504354/2	VIT_19s0014g05150 AAA+ ATPase/Resistance to P. syringae2-like *RPS2*	4528	-1.98	0.05	-0.27	0.78	aqc-miR482c-like self	6.5 0	2 3 2 2 3 2	0.008[b] 0.08[c] 0.13[d] 0.04[a] 0.004[c] 0.03[c]
408421/113	VIT_15s0046g02750 3 kb 5'; NB-ARC Potato virus X resistance-L	383	-1.16	0.38	-2.32	0.003	aqc-miR482c-like; "22_1"	6.5	0	0.01[d]
300691/135	VIT_12s0121g00050 MLA10 Resistance	634	-0.31	0.82	**2.57**	0.04	RPS2-5' D11(-)	5.5	3	0.10[c]
310368/55	VIT_12s0035g00410 NB-ARC Potato virus X resist-L	1289	-1.10	0.23	-1.12	0.04	RPS2-5' D11(-)	6.5	2	0.18[d]
340355/57	VIT_13s0139g00130 NB-ARC Potato virus X resist-L	1159	-1.68	0.05	-0.22	0.78	miR482 self	3.5 0	2 2	0.02[c] 0.03[d]
525156/25&167	VIT_19s0085g00460 83aa peptide	485.9	-2.92	0.01	**1.59**	0.20	miR3634 23 nt specie; down by XF other 83aa	3.5 0.5	3 2 0 3 3	0.06[d] 0.016[a] 0.001[b] 0.08[c] 0.06[d]
525163/36	VIT_19s0085g00480 83aa peptide	1336	-2.60	0.02	**0.11**	0.93	miR3634	3.5	4 0 3	0.03[a] .0008[b] 0.05[c]
525131/NA	VIT_19s0085g00430 54aa peptid	765.6	0.61	0.56	**0.19**	0.89	miR3634	2.5	0	.0007[b]
525162/119	VIT_19s0085g00470 70aa pept	901	-0.9	0.92	-0.79	0.38	miR3634	2.5	n.d.	
460578/45&115&189	VIT_18s0001g02000, Zn Finger	1758	-1.94	0.12	**0.15**	0.93	miR3634	3.5	0	0.002[a]

358178/3	VIT_14s0081g00100 57aa peptide; novel TAS[9]	9144	-2.91	0.02	**0.73**	0.40	miR7122-like "22_1"	4	2 2 3 2	0.005[a] 0.003[b] 0.03[c] 0.05[d]
79145/128	VIT_04s0008g04060 RD22 PHASI paralogs acting in *trans*: #144, 253	1256	N.A.	N.A.	**3.58**	N.A.	57aa-TAS-3'D16(+) PHAS#144 PHAS#253 self	5 0 2 0	2 3 3 3 2 3 3 2	0.07[a] 0.44[d] 0.03[a] 0.03[d] 0.14[a] 0.12[d] 0.03[a] 0.03[d]
79132/N.A.	VIT_04s0008g04040 BURP/RD22-like PHASI paralog acting in *trans*: #128,253	27.3	N.A.	N.A.	**0.14**	N.A.	57aa-TAS-3'D16(+) PHAS#253 PHAS#128	5.5 0 1	2 3 3 4 3	0.04[a] 0.03[d] 0.06[a] 0.06[b] 0.09[d]
490353/84 &122	VIT_18s0089g00510 IPT3-Like1 dimethylallyl tr-ase	~140	-1.56	0.16	**1.17**	0.11	unknwn			
160219/85	VIT_07s0104g00270 IPT3-Like2 dimethylallyl transferase	139	-2.87	0.02	-1.61	0.057	IPT3L1-D7(+) Self self	3 0 0	0 3 3	0.002[a] 0.009[c] 0.03[d]
229297/56	VIT_09s0070g00710 IPT3-Like3 dimethylallyl tr-ase	2338	-4.49	4E-04	-1.13	0.46	IPT3L1-D7(+) self	4 0	0 3	0.014[a] 0.03[d]
156350/NA	VIT_06s0080g00040 ABC transporterG-L1	168	5.46	1E-06	**5.20**	7E-07	unknwn L3 tasiD1	1	3	0.06[d]
155932/206	VIT_06s0061g01480 ABC transporterG-L2	209	3.71	0.001	**0.30**	0.79	self L3 tasiD1	0 4	3 3	0.08[a] 0.02[a]
155910/174	VIT_06s0061g01470ABCG-L3	183	5.92	2E-07	**5.55**	2E-07	self, 5' 838 nt	1.5	3	0.03[a]
400811/223	VIT_15s0021g02320 ABCG-L4	12.2	0.28	0.86	-2.05	0.08	PHASI 167D2?	3	3	0.96[d]
36236/246	Intergenic	12.1	-2.31	0.05	-1.80	5E-07	unknwn	N.A.		
110550/141	VIT_05s0020g04290 81aa pept	1404	-2.61	0.01	-0.05	N.A.	self	0	3	0.008[a]
404699/247	VIT_15s0048g02320 CUC2-like	56.5	-0.34	0.73	-1.97	0.003	unknwn	N.A.		
259366/236	VIT_10s0071g00060 148aa prot	297	0.17	0.86	**1.81**	0.06	unknwn	N.A.		

a. Downy mildew degradome; Brilli et al. (2018) [66].
b. Pantaleo et al. (2010) degradome [44].
c. pseudo-degradome; PD-symptomatic concatenated sRNA libraries
d. pseudo-degradome of concatenated public sRNA libraries

In addition to innate immune responses involving LRRs, pleiotropic PD symptoms like 'matchstick petioles' and 'cane bark' involve myriad physiological processes such as abnormal leaf blade abscission and lignification. We found that miR390 and miR393 decreased (albeit not significantly) as did the phasiRNAs from their targets *TAS3/AUXIN RESPONSE FACTOR3/4* and *TRANSPORT INHIBITOR RESPONSE*1/(*TIR1*). Because target mRNA abundances for miR393 targets *VIT_14s0068g01330/TIR1*, *VIT_05s0029g00390/Helix-loop-Helix*, and *VIT_14s0030g01240/TIR1-Like* increased in PD symptomatic leaves, this observation suggests a causal relationship of expression dynamics (**Table VII**) consistent with previous results supporting a role for these auxin effectors in bacterial disease etiology[55]. We also identified novel *TAS* genes annotated as 54aa/70aa/83aa and 57aa peptide-encoding transcripts triggered by 23 nt miR3634 and 22 nt species miR7122, respectively, and a *PHAS* gene encoding a Zinc Finger targeted by miR3634 (**Table VII**). Sun et al.[69] previously predicted the 70aa peptide as candidate target

for translational inhibition by miR3634. We also observed degradome-validated target mRNAs increased as miR3634 expression decreased in PD symptomatic libraries (albeit not significantly), where derived phasiRNAs decreased significantly for several of the short peptide transcripts (**Table VII**), consistent with a causal relationship underlying expression dynamics for this novel regulatory cascade.

The previously described miR7122 candidate target *TAS* locus[9] maps to a 2 kbp cluster of abundant (720 reads per million) sense- and antisense phasiRNAs spanning a 57aa peptide *VIT_14s0081g00100* . We found an atypical but suggestive miR7122 slicing event drawn from a recently published grape degradome library[66] on the 57aa-associated *TAS* transcript (*57aaTAS*), one nt shifted 3' on the mRNA from the canonical position 10 nt from the 5' end of the 22 nt miRNA. That this is a bona fide case of unusual slicing is substantiated by evidences from three other independent degradome and pseudo-degradome libraries for slicing at the expected position, with T plots showing the functional D16(+) and D17(+) 21 nt phasiRNAs remaining in respective register 315 and 336 nt downstream from the major trigger, respectively (data not shown). The 21 nt derived 3'D16(+) species (antisense to the 57aa transcript) sliced two PHAS loci encoding *RESPONSE TO DROUGHT22/RD22/BURP DOMAINs.* RD22 is a marker for resistance to the bacterium *Dickeya dadantii* (ex *Erwinia chrysanthemi*)[70] and previously 17 PHAS *RD22/BURP* paralogs in peach of unknown trigger provenance were described[61]. Although the complexity and high abundances of phasiRNAs at these loci preclude definitive proof that 57aaTAS-3'D16(+) species acts as primary determinant trigger, PhaseTank analysis documented phasing of 79 sense and 346 anti-sense siRNAs to the mRNA in registers 8-23 upstream in *RD22/VIT_04s0008g04060* and 53 sense siRNAs in 21 nt registers 1-6 downstream from the *RD22* slice site quantified by CleaveLand. 57aaTAS-5'D16(+) may be a 21_1 novel trigger comparable to miR828/TAS4/MYBA5/6/7 and distinct from the 22_2 and 22_1 models for miR7122 function in peach, strawberry, apple, and tobacco silencing *PENTATRICOPEPTIDE REPEATS/PPRs*[61]. Although mature and star duplexes for bona fide vvi-miR7122 and ppe-miR7122 have the same register (are not shifted isomiRs generated) from a conserved hairpin structure, the nucleotide conservation of the mature species is poor with seven mismatches between grape and peach; three mismatches are in the seed region that specifies function[71]. From these observations we conclude, supported by an absence of any PHAS locus originating from PPRs found in the ~230 PHAS loci, that PPRs are not targeted by miR7122 in grapevine. Mirroring the observed expression dynamics of down regulation of miRNAs and up regulation of mRNAs listed in **Table VI**, other PHAS loci of unknown triggers were identified with strongly up- or down-regulated phasiRNAs and/or mRNAs. These included several *PLEIOTROPIC DRUG RESISTANCE/ABC-G* transporter family members homologous to *ABCG2/20* regulated in Arabidopsis by natural cis-antisense RNAs[72] and which function in suberin production[73] and nutrient uptake[74]. Other orphan PHAS loci included *VIT_10s0071g00060* encoding an unknown 148aa peptide and several paralogs of nuclear-localized cytokinin biosynthesis enzymes *VIT_18s0089g00510/ISOPENTENYL TRANSFERASE3-Like1*, (**Table VII**).

Independent evidences supporting the model: Two studies previously documented mis-regulation of *MFS/SPX1* (target of miR827) in response to 8 weeks XF incubation in grapevine[58] and at 9 days post-XF infection in Arabidopsis[59]. *NITROGEN LIMITATION ADAPTATION* and close homologues in Arabidopsis, dicots and monocots are known to encode MFS-RING-finger-type ubiquitin E3 ligases and/or P_i translocators targeted by miR827[48] that function in phosphate signaling in conjunction with miR399-targeted E2 conjugase *PHO2*. PHO2 directs 26S proteasome ubiquitin-mediated degradation of a family of membrane-localized MFS phosphate translocators called PHTs[48, 49]. Grapevine phosphate transporter *VvPHT2;1* was shown previously to be significantly down-regulated eight weeks after XF infection[58]. Reduced activities of miR399/827 in response to XF predicts that *VvPHT5/NLA-like* target *VIT_07s0005g00280* would increase (**Fig. 8**); we indeed observe significant up-regulation of this gene (LFC=2.18, *P*adj < 0.0005; data not shown) and validated[9, 44] phasiRNA-producing (**Table VI**) miR828 target MYB *PROANTHOCYANIDIN3-like VIT_09s0002g01380* (LFC= 2.19, *P*adj= 0.03). **These results strongly support the hypothesized molecular mechanisms**. Based on their mobile nature (aka 'diffusible signal factors') in vascular tissues, P_i, sugars, hormones (ABA), miRNAs and target mRNAs have been recognized as systemic signals that convey the whole-plant P_i status internally[48, 75, 76], whereas endomembrane bound Ca^{2+} transporters (target of miR391/3627)[9] have also been implicated in systemic P_i signaling[57] and induction of *CHALCONE SYNTHASE*[47], supporting our dynamic model directly relevant to the XF growth habit, symptoms, and providing insight to the prior claim that XF infection results in increases in leaf calcium[4].

Concordant (instead of canonical predicted inverse) changes in miRNAs and their targets has been observed in rice[77], Arabidopsis[6], and recently by us for UV-B regulated grape miRNAs[9], supporting the model that the miR828, -827, and -399 circuits are under complex regulation (e.g. autoregulation). We also confirmed in grape[9] the findings in

soybean[67, 78] that miRNA biogenesis effectors *DCL2* and *SUPPRESSOR_OF_GENE_SILENCING3* (*SGS3*) are subject to PTGS resulting in phasiRNA accumulation, as are *ARGONAUTE2* and *AGO2-Like* which is novel (**Table VI**). ***These data-driven findings constitute 'smoking guns' that validate and refine our model that other sRNA regulons and RNAi amplification are involved in XF pathogenesis, in addition to the pioneering case of* MIR828/TAS.** Taken together, these systems analyses clustering of gene ontology in our RNA-Seq and sRNA-Seq data ***very strongly support the working model.*** A revised molecular working model focusing on dynamics of candidate miRNA target pathways (miR828, -399, -827, -397/408; **Table VI**) based on our results is shown in **Fig. 8**.

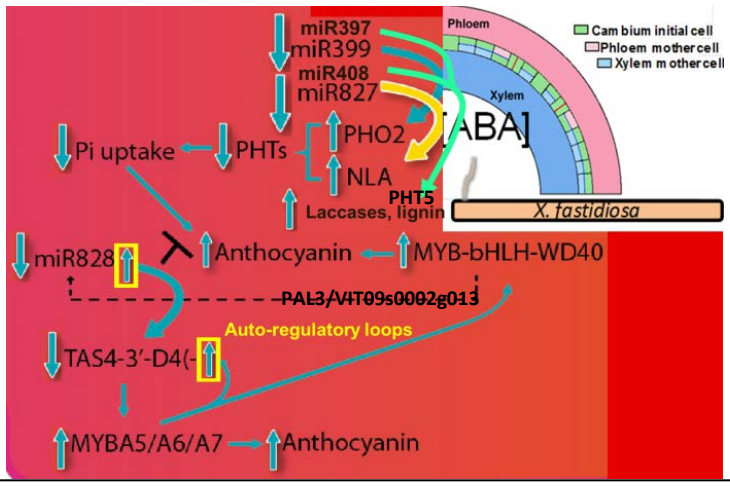

Fig. 8. Working model, taking into account the role of miR828/TAS4 autoregulatory loops and other phosphate starvation-induced miR399/miR827/ miR408 identified empirically as significantly down-regulated by XF infections in field samples taken from Temecula CA 2015-2017.

Summary of Objective II accomplishments

sRNA-seq and mRNA-Seq identified tobacco genes involved in anthocyanin synthesis and phosphate-regulated miRNAs modulated by XF infection. Genome-wide analysis of differentially expressed miRNAs and small-interfering RNAs in XF-infected PD symptomatic grape samples from the field showed significant down-regulation by XF infection of phosphate-associated miR858, miR828/TAS4b, miR391/3627, miR827, miR399, miR397, and miR408. In greenhouse-grown tobacco miR828/TAS4b, miR399, miR166 were downregulated and miR827, miR156, miR319/miR159 were upregulated upon XF infection. Systems analysis of RNA-seq and sRNA-seq from XF-infected samples showed inverse concordant up-regulations of some mRNAs encoding degradome-validated miRNA/siRNA slicing targets, namely MYB transcription factor effectors of flavonols, proanthocyanidins and anthocyanins, a Ca^{2+} transporter *ACA10*, phosphate homeostasis regulators/transporters, and laccases involved in lignin biosynthesis. Our results strongly support the working hypothesis that XF exploits host miRNAs as a 'Trojan horse' to circumvent or derange innate pathogen immunity responses and cause pleiotropic disease symptoms.

III. Characterize the changes in control versus edited genotypes for (a) xylem sap [Pi], and (b) polyphenolic levels of XF-infected canes and leaves. If results are conclusive based on greenhouse studies, in the future we will conduct field trials and collaborate to carry out insect diet preference/behavioral modification/fitness assays on defended transgenic materials. (c) Test the Pi analogue Phi as a durable, affordable and environmentally sound protectant/safener for PD.

Objectives IIIa,b. We previously reported in the July 2017 Interim Progress Report for completed project #15-0214SA results for mass spectrometric quantification of cyanin and malvin in xylem sap from the Temecula June 2017 field samples, and anthocyanins in leaves, showing significant differences between infected and control samples for the latter. We also showed P_i quantifications by two methods on leaves and canes in 2016 and 2017 Temecula PD samples. Results support the hypothesis that XF infection results in significantly lower [P_i] (about 60% decrease) in host leaves and xylem sap that correlate with elevated anthocyanins in XF-infected xylem sap and leaves. These results are further substantiated by prior results for other grape cultivars[79, 80], supporting the working model. We have

generated results for XF titers in concordant petioles samples from those same prior leaf samples by real time-PCR, as well as for the 2016 replicated greenhouse XF tobacco MYB90 overexpression experiment. **Table VIII** shows the results correlated with digital abundances of XF transcriptome reads from Objective II new analyses quantified by bowtie[81]. The results directly support the hypothesis that XF infection results in accumulation of anthocyanins in xylem sap and leaves. Thus we have accomplished Obj. IIIb and are publishing the results. Similar results have been reported for procyanidins and other polyphenolics in xylem sap two months post-XF infection in Thompson seedless and several winegrape cultivars[79, 80]. Phenolic levels in Merlot cv xylem sap correlate with PD severity compared to other cultivars[82].

Table VIII. Quantification of XF titers by quantitative real-time PCR and RNA-seq in 2016 greenhouse replicated XF challenge experiment with AtMYB90-overexpressing transgenic tobacco, and Temecula CA 2017 field samples.

Sample	**Log_{10}, cfu/gfw qRT-PCR (± s.e.m.)**	**Leaf XF RNA-seq Reads/10^6 host reads**	***P*- value**
Control leaf petioles, 2017 Temecula	5.21 (0.17)	1.8 (n=2)	---
PD symptom leaf petioles, 2017 Temecula	6.82 (0.40)	10.2 (n=1)	0.006*****
SRI non transgenic-Buffer control	7.30	3.0	
Hemizygous transgenic-Buffer	7.30	0	
Homozygous transgenic-Buffer	7.32	0.8	
SRI non transgenic-XF infected	12.4	88	
Hemizygous transgenic-XF infected	12.0	129	
Homozygous transgenic-XF infected	12.1	299	0.03†

* significantly different from qRT-PCR control, Student's two-sided t-test, n=5, equal variance assumed.
† significantly different from RNA-Seq buffer controls, Student's one-sided t-test.

Supporting our previous results that XF infection induces miR828 and *TAS4* expression in tobacco, **Figure 9** shows a blot probed with the transgene of RNA extracted from the 2106 repeat greenhouse XF challenge experiment that further establishes the importance of the autoregulatory feedback loop in XF host response based on PAP2/AtMYB90 induction upon XF infection, because even in the absence of the transgene (the SR1 non-transgenic control line) the endogenous PAP2/MYB90 orthologue *ANTHOCYANIN2* is inferred to hybridize with the probe due to high homology with *PAP2/MYB90*.

As an independent, partial test of the hypothesis, we utilized transgenic tobacco that overexpresses the Arabidopsis target of *TAS4* siRNA; *AtMYB90/PRODUCTION OF ANTHOCYANIN PIGMENT2/PAP2*. Transgenic plants have a dominant phenotype of purple leaves[83] and functional endogenous Nta-miR828[84] and *NtTAS4ab*[8] expression hypothesized to interact with the transgene[85]. **Figure 9** shows conclusive evidence, as previously shown in Arabidopsis[5, 6], for functional conservation of an autoregulatory loop involving tobacco orthologue of *AtMYB90*, *ANTHOCYANIN2/AN2*, where XF infection induces *AN2* and *AtMYB90*/*PAP2* overexpression which in turn induce expression of the endogenous negative siRNA regulator Nt*TAS4*-3'D4(-) and its upstream trigger Nt-miR828. The result clearly shows *AN2* to be up-regulated several fold in the SR1-treated sample in response to XF infection. Remarkably, both Nt-TAS4 D4(-) and Nt-miR828 are paradoxically down-regulated by XF infection, which is interpreted as XF having a causal role in disease etiology because it both ***activates the positive effectors*** of anthocyanin (AN2, MYB90) and ***represses the downstream negative regulators*** *TAS4* and miR828. The inverse correlations observed between both *Nt-TAS4*-3'D4(-), Nt-miR828, and XF infection status in *PAP2*-overexpressing tobacco genotypes is strong evidence in support of our model. Consistent with the *causative* XF model and a key role for XF impacting the autoregulatory loop, quantitation of anthocyanins and disease severity of leaf scorching in XF-infected tobacco genotypes show Nt*TAS4*-3'D4(-) and Nt-miR828 reductions (**Fig. 9**) correlate with leaf anthocyanin reductions and disease symptom severity (**Fig. 10**). Taken together, these results suggest that infection both turns on the anthocyanin pathways and dampens negative effectors of pathway. Ultimately high transgene activities correlate with overall reductions in anthocyanins and disease symptom severity.

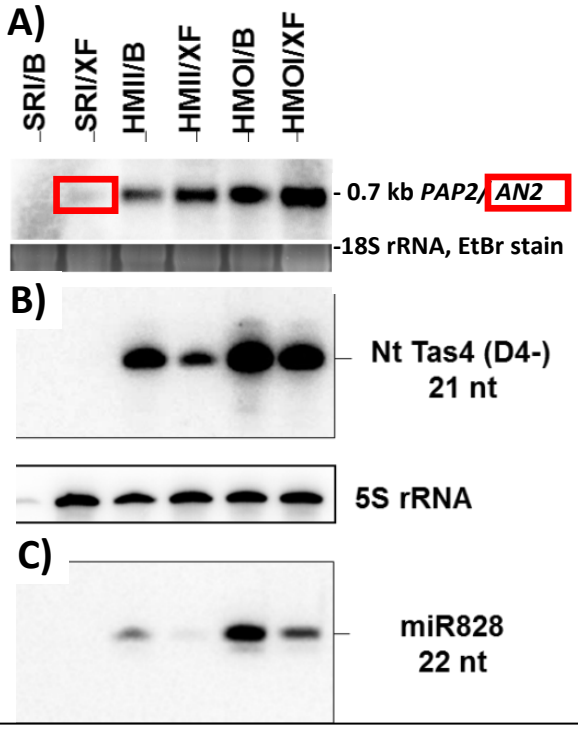

Fig. 9. Molecular evidence from transgenic tobacco overexpressing PAP2/MYB90 supporting that XF infection deranges a conserved endogenous tobacco miR828/*TAS4/MYB-AN2* autoregulatory loop. **A)** XF infections induce expression of AN2 orthologue of PAP2/MYB90 (red box) and transgene PAP2. **B)** Endogenous *TAS4*-3'D4(-) and **C)** miR828 abundances are decreased by XF infection in *AtMYB90*-overexpressing tobacco genotypes. miR828 and *TAS4*-3'D4(-) expressions in transgenics correlate with reproducible disease severity symptoms and anthocyanin reductions (not shown) supporting XF disease model. Overexpression of *AtMYB90* induces miR828 and D4(-), demonstrating functional conservation of autoregulatory loop [58, 59, 61]. B: buffer. XF: infected 7 weeks. SR1: control non-transgenic. Hmi: hemizygous *AtMYB90* transgene. Hmo: homozygous *AtMYB90* transgene.

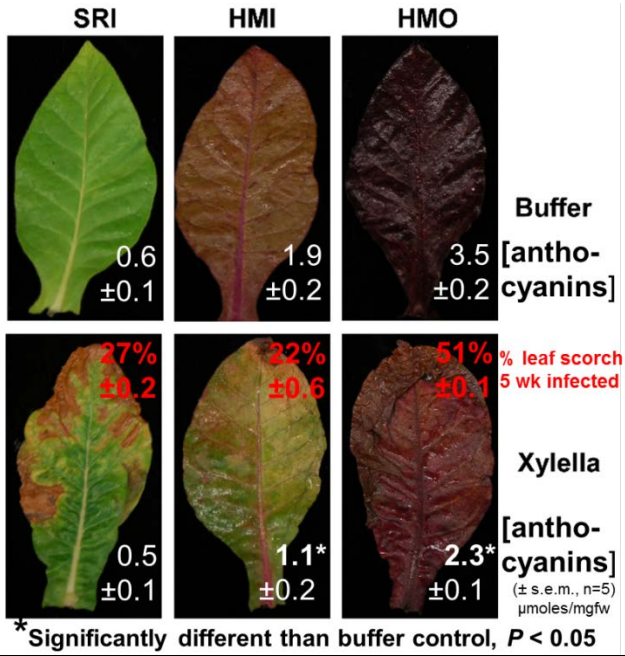

Fig. 10. Further evidence supporting hypothesis of miR828/TAS4/MYBs as nexus for PD: XF infection of tobacco over-expressing *TAS4* target *PAP2*/*MYB90* causes reduced anthocyanins. Overexpression gene copy number correlates with more severe disease symptoms in greenhouse XF challenge experiments.

These results together directly support the hypothesis that XF infection results in accumulation of anthocyanins in xylem sap and leaves. Thus we have accomplished Obj. IIIa/b and have submitted the results for publication.

Objective IIIc P_i analogue Phi as a protectant/safener for PD.

We showed results in the Final Report 15-0214-SA validating the LD_{50} < 3 mM [Phi] for inhibition of plate growth of XF. Based on pilot experiments conducted at the end of previous project #15-0214SA, we conducted a greenhouse XF challenge experiment from April until July 2018 with phosphite treatments as test. We encountered technical problems with 1) plant growth in the absence of fertigation (we did not want phosphite effects to be confounded by excess nutrient conditions and thus withheld application of NPK fertigation), and 2) with the third time point (experiment endpoint) RT-PCR XF titer assay that required us to repeat the experiment twice. Below is described the results for the first repeat experiment with five tobacco plants of each genotype (SR1 non-transgenic, HMI heterozygous transgenic, and HMO homozygous transgenic overexpressing AtPAP2/MYB90[83, 85]) challenged with XF in the greenhouse. The results in **Table IX** demonstrated the technical methods and experimental procedures give reproducible results in our hands, because we validate and extend the prior results documented in the Feb. 2016 Progress Report that the transgenic lines have lower XF titers that correlate with transgene copy number, yet higher leaf scorch symptom severity in the homozygous transgenic line. We conducted a larger phosphite test for XF antagonism in winter 2018 (**Fig. 11**) using three genotypes, six control replicates per genotype, and three test replicates bracketing the parameters of phosphite concentrations administered by foliar spray or irrigation, and interaction with a phosphorus fertigation supplement during post-inoculation growth and development (n= 72 individual plants). **Figure 11 inset** shows evidence that support our prior findings, from the 2015 and 2016 repeat XF challenge experiments, that disease severity correlates with the more heavily pigmented homozygous transgenic lines (HMO), which show significant decreases in anthocyanins compared to uninfected control genotype in response to XF challenge. The principal results of this larger repeat experiment are shown in **Figure 12**. It is concluded that the XF challenge conditions were optimal and showed highly significant results (**Fig. 12A-C**) for all three genotypes compared to inoculum buffer alone ($P < 10^{-8}$, two sided Student's t-test, equal variance assumed). However, despite a clear trend that phosphite treatments inhibited XF growth in planta, especially the spray treatment, the number of biological replicates (three) per variable tested were insufficient to establish cause and effect of phosphite treatments on XF titers (**Fig. 12D**). If funding had continued, we are confident we would have been able to accomplish Objective IIIc and draw conclusions for phosphite sprays as a durable XF safener by repeating the greenhouse XF challenge experiment with a larger design on fewer select genotypes tested by more replicates.

Table IX. Results of XF challenge of greenhouse-grown transgenic tobacco plants (n=5) overexpressing AtPAP2/MYB90 assayed at two and seven weeks post infection (WPI) for bacterial titer by RT-PCR.

Genotype	**2 WPI**	**7 WPI**	**p value† vs control, 2 WPI**
	cfu/gfw		
SR1 non transgenic	2.3E+07	3.0E+09	--
HMI heterozygous transgenic	6.4E+06	2.1E+07	0.07
HMO homozygous transgenic	5.6E+06	9.4E+06	0.05

† two sided Student's t-test, unequal variance assumed

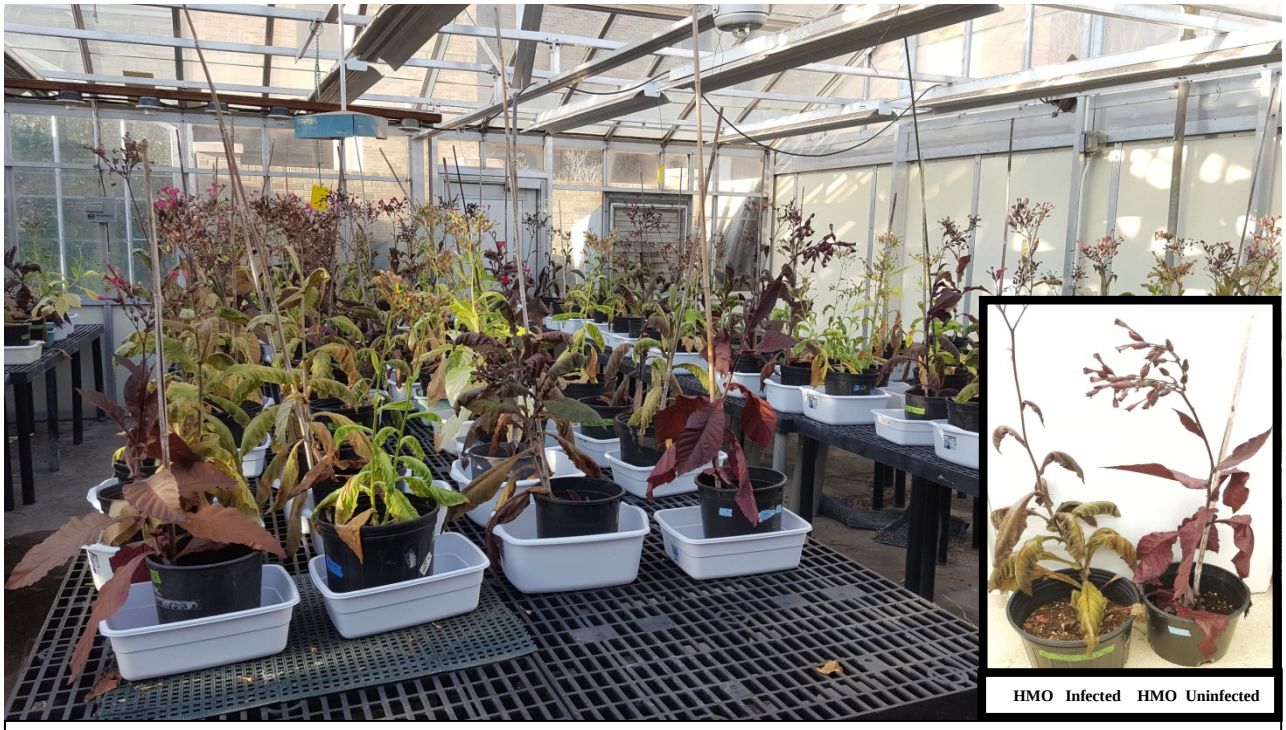

Fig. 11. Ongoing greenhouse XF challenge experiment for Phi as safener/protectant against PD. *Inset*: XF-infected transgenic homozygous plants over-expressing AtMYB90 have reduced anthocyanin and more severe symptoms.

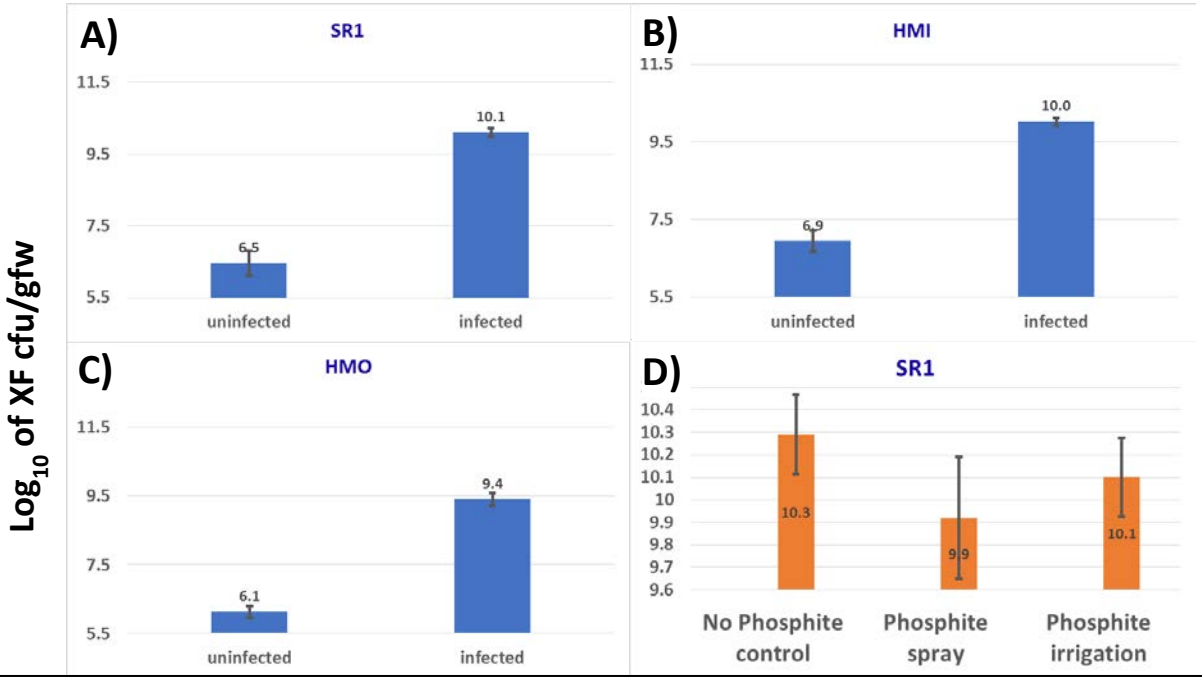

Fig. 12. Main results of large XF challenge experiment testing phosphite as durable safener to protect tobacco transgenic genotypes from infection spreading. A- C) Highly reproducible > 1,000-fold XF colony forming unit (cfu) increases in response to prick inoculation across three genotypes tested: non-transgenic SR1 (A), heterozygous *AtMYB90* overexpressing HMI (B), and homozygous *AtMYB90* overexpressing HMO (C). D) Trend of reduced XF titers in response to phosphite treatments in SR1 genotype. n= 6-18 replicates for A-C; n= 3 replicates for D. Overall significance of A-C test results: $P < 10^{-27}$ (n=18-72; two sided t-test).

Summary of Objective III accomplishments
These results together further support our claim substantiated in prior reports that XF infection directly or indirectly impacts host anthocyanin metabolism, consistent with the working hypothesis and results of Objective II. We obtained supporting evidence for both tobacco and grapevine autoregulatory miR828/TAS4/MYB loops being down-regulated by XF infection from sRNA blots of Vv-TAS4-3'D4(-) and miR828 expression in leaves from CA and GA field-grown vines manifesting PD symptoms. The visible phenotypes (**Fig. 11 inset**) and molecular signatures (Obj. II) are conclusive evidence, as previously shown in grapevine[8], for functional conservation of an autoregulatory loop[5, 6] involving tobacco *AtPAP2/MYB90* orthologue *AN2*, where XF infection induces *AN2* expression (and *AtMYB90*/*PAP2* over-expression), which trans-activates expression of the endogenous negative anthocyanin siRNA regulators Nt-*TAS4ab*-3'D4(-) and their upstream triggers nta-miR828ab. Remarkably, both Nt-TAS4-3'D4(-) and nta-miR828 are paradoxically down-regulated by XF infection in transgenic plants, which is interpreted as XF having a *causal* role in disease etiology because it both *activates* the positive effectors of anthocyanin (AN2, MYB90) while *repressing* the downstream negative regulators *TAS4* and miR828.

PUBLICATIONS AND PRESENTATIONS MADE THAT RELATE TO THE FUNDED PROJECT
Reverse chronology

Sunitha S, Rock CD "CRISPR/Cas9-mediated targeted mutagenesis of *TAS4b* and *MYBA7* genes in grapevine rootstock 101-14." *Transgenic Research* ms #TRAG-D-19-00076, under review.

Sunitha S, Azad MF, Traore S, De La Fuente L, Rock CD. "microRNAs associated with phosphate starvation and secondary metabolism are down-regulated in *Xylella fastidiosa*-infected grapevine." Under revision from *Plant Cell* submission #TPC2019-RA-00188.

Sunitha S, Rock CD, Azad MF, Tricoli D, De La Fuente L, Traore S. "A conserved autoregulatory feedback loop is targeted by grape pathogens." Plant-2019: International Conference on Plant Science Research. March 4-5, 2019. DoubleTree by Hilton Baltimore BWI Airport. Oral presentation.
https://unitedscientificgroup.com/conferences/plant/whova.html

Sunitha S, Loyola R, Alcalde JA, Arce-Johnson P, Matus JT, Rock CD (2019) The role of UV-B light on small RNA activity during grapevine berry development. *G3: Genes|Genomes|Genetics* 9: 769-787. This paper is not directly related to the project, but lays the groundwork for Objective II with baseline characterization of host miRNAs regulated during berry development and in response to abiotic light and oxidative stresses. The work was funded by FAPESP-SPRINT Brazilian-TTU Joint Program and TTU-VPR Open Access Publication Initiative awards to the PI.

Rock CD, Sunitha S, Azad MdF, Tricoli D. "Genome editing of *TAS4*, *MIR828*, and targets *MYBA6/A7*: A critical test of *Xylella fastidiosa* infection and spreading mechanisms in Pierce's Disease." 2018 CDFA Pierce's Disease Research Symposium Proceedings. Pp. 66-81. Dec. 17-19, 2018. Kona Kai Resort, San Diego, CA. Oral presentation.
https://www.cdfa.ca.gov/pdcp/Documents/Proceedings/2018ResearchProgressRpts.pdf

Rock CD. "Career opportunities in agricultural genomics and genetics." Agronomy Society Field Day keynote oral presentation. July 6, 2018. Brigham Young University-Idaho, Rexburg, ID. Presented project progress in context of potential impacts on Idaho winegrape and potato production. (Potato is infected by both XF and a different bacterium [Candidatus Liberibacter solanacearum]; both bacteria are associated with "Zebra Chip" and "purple top" maladies).

Rock CD, Azad F, Sunitha S, Maia I, Nunes-Laitz AVN, Domingues D. "The auto-regulatory loop involving miR828, *TAS4*, and target MYB transcription factors: basic and applied studies." Sao Paulo Research Foundation (FAPESP)-TTU Conference: "SPRINT STEM Across Continents." TTU International Cultural Center, Lubbock TX. Sept. 21, 2017. Oral presentation.

Rock CD. (2017) Phenylpropanoid metabolism. In: eLS (Encyclopedia of Life Science). John Wiley & Sons, Ltd: Chichester. DOI: 10.1002/9780470015902.a0001912.pub2

Rock CD, Azad F, Sunitha S, Traore SM, De La Fuente L, Tricoli D. "Genome editing of *TAS4*, *MIR828*, and targets *MYBA6/A7*: A critical test of *Xylella fastidiosa* infection and spreading mechanisms in Pierce's disease." 2017 CDFA Pierce's Disease Control Program Symposium Proceedings. Pp. 70-78.
https://www.cdfa.ca.gov/pdcp/Documents/Proceedings/2017CDFAWinegrapePestResearchRpts.pdf

Rock CD, Azad F, Sunitha S, Traore SM, De La Fuente L, Tricoli D. "Genome editing of *TAS4*, *MIR828*, and targets *MYBA6/A7*: A critical test of *Xylella fastidiosa* infection and spreading mechanisms in Pierce's disease." 2016 CDFA Pierce's Disease Control Program Symposium Proceedings. Dec. 12-14, 2016. Pp. 121-129. Courtyard San Diego Liberty Station Hotel, San Diego CA. Oral presentation.
https://www.cdfa.ca.gov/pdcp/Documents/Proceedings/2016ResearchProgressRpts.pdf

Rock CD, De La Fuente L, Sunitha S, Traore SM. "Genome editing of *TAS4*, *MIR828*, and targets *MYBA6/A7*: A critical test of *Xylella fastidiosa* infection and spreading mechanisms in Pierce's disease." 2015 CDFA Pierce's Disease Control Program Symposium Proceedings. Pp. 164-170.
https://www.cdfa.ca.gov/pdcp/Documents/Proceedings/2015ResearchProgressRpts.pdf

U.S. Patent application #61,641,045 (filed 05/1/12) converted to regular application #13874962 (filed 05/01/13) "Regulating plant development and secondary metabolite biosynthesis useful for e.g. treating Pierce's disease due to *Xylella fastidiosa* infection by providing plant cells with anthocyanin effector, and regulating expression of genes" by C.D. Rock and Q.-J. Luo. USPTO Application published 3/13/14 Publication No. US-2014-0075596-A1. Texas Tech University Office of Technology Commercialization Docket # TTU D-0862, D-0876, D-1327, and 2019-075.

RESEARCH RELEVANCE STATEMENT, INDICATING HOW THIS RESEARCH WILL CONTRIBUTE TOWARDS FINDING SOLUTIONS TO PIERCE'S DISEASE IN CALIFORNIA.

Our novel results demonstrating that Phi impacts XF growth underscores the practical value of the project to develop a durable management tool while generating new knowledge about PD etiology and engineered resistance. The Board has suggested knocking out genes involved in diffusible signals and host chemical specificity for PD etiology by CRISPR (pp. A1-3); this is precisely what the PI has accomplished. Knocking out any host gene (e.g. PD resistance or P stress effector) may result in increased susceptibility to infections. Thus engineering PD resistance is likely to be by incremental advances from characterizing necessity and sufficiency of gene functions implicated as effectors of PD disease states by creating genome-edited knockout alleles of potential practical value.

LAYPERSON SUMMARY OF PROJECT ACCOMPLISHMENTS

We have generated conclusive evidence supporting our working hypothesis that inorganic phosphate (P_i)-regulated microRNAs (miRNAs) mediate pleiotropic PD symptoms by deranging host Post-Transcriptional Gene Silencing mechanisms including amplification by miR828-triggered production of phased small-interfering RNAs (phasi-RNAs) targeting MYBA5/6/7 transcription factors that control anthocyanin biosynthesis. We have been successful at making inroads into understanding molecular mechanisms and have submitted the work to date for review by the premier international journal *The Plant Cell*. We have also filed an invention disclosure to our institution on enablement via genome editing technology of a pending patent application that claims *MIR828*, *TAS4*, and *MYB* targets. Recently the USDA issued a directive that the agency does not have plans to regulate plants generated using gene editing techniques that create deletions/insertions that could otherwise have been developed through traditional breeding techniques and are not developed using plant pests as donor (except complete null segregants which are exempt, like those produced by outcrossing as envisioned for future deployment). This development provides a path for commercialization of value-added genome-edited grapevine without expensive regulatory proscriptions.

STATUS OF FUNDS

Funds were expended on track as budgeted.

SUMMARY AND STATUS OF INTELLECTUAL PROPERTY ASSOCIATED WITH THE PROJECT:

The PI has disclosed a "Subject Invention" (USPTO patent application #13/874,962; May 1, 2013). As described in the July 2016 CDFA Progress Report for 15-0214-SA, the PI disclosed to his institution (Docket D-1327, Sept. 18, 2016) the enabling sequences that form the basis of a Continuation in Part for original claims 12-21 subject to rejoinder as indicated in Manual of Patent Examining Procedure § 821.01 through § 821.04. On March 19, 2019 the PI and collaborator Sunitha Sukumaran filed invention disclosure #2019-075 to their institution on enablement of claims 12-21 of the patent application. If title is elected TTU will share reagents via a Materials Transfer Agreement. Interested parties are referred to David Snow, Director and IP Manager, www.texastech.edu/otc, ph. 806-834-4989. For commercialization of transgenic dicot plants, including grapevine made by the Agrobacterium co-cultivation method, the patent (USPTO# 8273954) will need to be licensed from Monsanto for industrial partners to have freedom to operate.

CRISPR/Cas9 foundational technologies have been successfully prosecuted for patent protection by inventors at UC Berkeley (UCB)/University of Vienna (PCT/US2013/032589; priority date May 25, 2012; USPTO#10,000,772 issued 6/19/18) and Massachusetts Institute of Technology (MIT) (USPTO# 8697359, issued 4/15/14 and approved 2017). The US Court of Appeals ruled on 9/10/18 in an infringement suit brought by UCB against MIT that both patents are upheld, ruling that both groups' use of CRISPR were different and "non-obvious." The implication is that there is a reasonable expectation that CRISPR would not work in plants, and that future plant CRISPR applications will be inventions subject to patent protection. Companies wishing to practice the CRISPR/Cas9 technology can negotiate non-exclusive licenses from The Broad Institute/MIT and from Caribou Biosciences (www.cariboubio.com). Non-exclusive licenses are also available for other CRISPR-based patents.

LITERATURE CITED

1. Thorne ET, Stevenson JF, Rost TL, Labavitch JM, Matthews MA. (2006) Pierce's disease symptoms: comparison with symptoms of water deficit and the impact of water deficits. *Amer J Enol Vitic* 57:1-11
2. Saponari M, Boscia D, Altamura G, Loconsole G, Zicca S, D'Attoma G et al. (2017) Isolation and pathogenicity of *Xylella fastidiosa* associated to the olive quick decline syndrome in southern Italy. *Sci Rep* 7:17723
3. Pierce NB: (1892)The California vine disease. Bulletin No. 2. Division of Vegetable Pathology. : U.S.D.A. Washington, D.C. 222 pp.
4. De La Fuente L, Parker JK, Oliver JE, Granger S, Brannen PM, van Santen E et al. (2013) The bacterial pathogen *Xylella fastidiosa* affects the leaf ionome of plant hosts during infection. *PLoS ONE* 8:e62945
5. Luo Q-J, Mittal A, Jia F, Rock CD. (2012) An autoregulatory feedback loop involving *PAP1* and *TAS4* in response to sugars in Arabidopsis. *Plant Mol Biol* 80:117-129
6. Hsieh LC, Lin SI, Shih ACC, Chen JW, Lin WY, Tseng CY et al. (2009) Uncovering small RNA-mediated responses to phosphate deficiency in Arabidopsis by deep sequencing. *Plant Physiol* 151:2120-2132
7. Zhao H, Sun R, Albrecht U, Padmanabhan C, Wang A, Coffey MD et al. (2013) Small RNA profiling reveals phosphorus deficiency as a contributing factor in symptom expression for citrus Huanglongbing disease. *Mol Plant* 6:301-310
8. Rock CD. (2013) *Trans-acting small interfering RNA4*: key to nutraceutical synthesis in grape development? *Trends Plant Sci* 18:601-610
9. Sunitha S, Loyola R, Alcalde JA, Arce-Johnson P, Matus JT, Rock CD. (2019) The role of UV-B light on small RNA activity during grapevine berry development. *G3: Genes|Genomes|Genetics* 9:769-787
10. Jacobs T, LaFayette P, Schmitz R, Parrott W. (2015) Targeted genome modifications in soybean with CRISPR/Cas9. *BMC Biotechnology* 15:16
11. Tricoli D, Chi-Ham C, Prieto H. (2014) Development of a grape tissue culture and transformation platform for the California grape research community. *Proceedings, 2014 Pierce's Disease Research Symposium. California Department of Food and Agriculture, Sacramento, CA.* 211-219. available online at https://www.cdfa.ca.gov/pdcp/research.html
12. Zhu X, Xu Y, Yu S, Lu L, Ding M, Cheng J et al. (2014) An efficient genotyping method for genome-modified animals and human cells generated with CRISPR/Cas9 system. *Sci Rep* 4:6420
13. Jacobs TB, Martin GB. (2016) High-throughput CRISPR vector construction and characterization of DNA modifications by generation of tomato hairy roots. *J Vis Exp: JoVE*; e53843, doi:53810.53791/53843

14. Belhaj K, Chaparro-Garcia A, Kamoun S, Nekrasov V. (2013) Plant genome editing made easy: targeted mutagenesis in model and crop plants using the CRISPR/Cas system. *Plant Meth* 9:39
15. Raitskin O, Patron NJ. (2016) Multi-gene engineering in plants with RNA-guided Cas9 nuclease. *Curr Opin Biotechnol* 37:69-75
16. Jia H, Orbovic V, Jones JB, Wang N. (2015) Modification of the PthA4 effector binding elements in Type I CsLOB1 promoter using Cas9/sgRNA to produce transgenic Duncan grapefruit alleviating XccΔpthA4:dCsLOB1.3 infection. *Plant Biotech J* 14:1291-1301
17. Nakajima I, Ban Y, Azuma A, Onoue N, Moriguchi T, Yamamoto T et al. (2017) CRISPR/Cas9-mediated targeted mutagenesis in grape. *PLoS ONE* 12:e0177966
18. Wang X, Tu M, Wang D, Liu J, Li Y, Li Z et al. (2018) CRISPR/Cas9-mediated efficient targeted mutagenesis in grape in the first generation. *Plant Biotech J* 16:844-855
19. Ren C, Liu X, Zhang Z, Wang Y, Duan W, Li S et al. (2016) CRISPR/Cas9-mediated efficient targeted mutagenesis in Chardonnay (*Vitis vinifera* L.). *Sci Rep* 6:32289
20. Daugherty MP, Rashed A, Almeida RPP, Perring TM. (2011) Vector preference for hosts differing in infection status: sharpshooter movement and Xylella fastidiosa transmission. *Ecol Entomol* 36:654-662
21. Almeida RPP, Nunney L. (2015) How do plant diseases caused by *Xylella fastidiosa* emerge? *Plant Dis* 99:1457-1467
22. Bray NL, Pimentel H, Melsted P, Pachter L. (2016) Near-optimal probabilistic RNA-seq quantification. *Nat Biotech* 34:525-527
23. Gamir J, Pastor V, Kaever A, Cerezo M, Flors V. (2014) Targeting novel chemical and constitutive primed metabolites against *Plectosphaerella cucumerina*. *Plant J* 78:227-240
24. Camañes G, Pastor V, Cerezo M, García-Agustín P, Flors Herrero V. (2012) A deletion in the nitrate high affinity transporter NRT2.1 alters metabolomic and transcriptomic responses to *Pseudomonas syringae*. *Plant Sig Behav* 7:619-622
25. Anders S, Huber W. (2010) Differential expression analysis for sequence count data. *Genome Biol* 11:R106
26. Jagadeeswaran G, Saini A, Sunkar R. (2009) Biotic and abiotic stress down-regulate miR398 expression in Arabidopsis. *Planta* 229:1009-1014
27. Kalvari I, Argasinska J, Quinones-Olvera N, Nawrocki EP, Rivas E, Eddy SR et al. (2018) Rfam 13.0: shifting to a genome-centric resource for non-coding RNA families. *Nucl Acids Res* 46:D335-D342
28. Jaillon O, Aury J, Noel B, Policriti A, Clepet C, Casagrande A et al. (2007) The grapevine genome sequence suggests ancestral hexaploidization in major angiosperm phyla. *Nature* 449:463-467
29. Kozomara A, Griffiths-Jones S. (2014) miRBase: annotating high confidence microRNAs using deep sequencing data. *Nucl Acids Res* 42:D68-D73
30. Pimentel HJ, Bray N, Puente S, Melsted P, Pachter L. (2017) Differential analysis of RNA-Seq incorporating quantification uncertainty. *Nat Meth* 14:687-690
31. Zaini PA, Nascimento R, Gouran H, Cantu D, Chakraborty S, Phu M et al. (2018) Molecular profiling of Pierce's Disease outlines the response circuitry of *Vitis vinifera* to *Xylella fastidiosa* infection. *Front Plant Sci* 9:771
32. Usadel B, Poree F, Nagel A, Lohse M, Czedik-Eysenberg A, Stitt M. (2009) A guide to using MapMan to visualize and compare Omics data in plants: a case study in the crop species, maize. *Plant Cell Environ* 32:1211-1229
33. Love MI, Huber W, Anders S. (2014) Moderated estimation of fold change and dispersion for RNA-seq data with DESeq2. *Genome Biol* 15:550
34. Jiu S, Leng X, Haider MS, Dong T, Guan L, Xie Z et al. (2019) Identification of copper (Cu) stress-responsive grapevine microRNAs and their target genes by high-throughput sequencing. *Roy Soc Open Sci* 6:180735
35. Zhu H, Xia R, Zhao BY, An YQ, Dardick CD, Callahan AM et al. (2012) Unique expression, processing regulation, and regulatory network of peach (*Prunus persica*) miRNAs. *BMC Plant Biol* 12:18
36. Xia R, Zhu H, An Y-q, Beers E, Liu Z. (2012) Apple miRNAs and tasiRNAs with novel regulatory networks. *Genome Biol* 13:R47
37. Klevebring D, Street N, Fahlgren N, Kasschau K, Carrington J, Lundeberg J et al. (2009) Genome-wide profiling of Populus small RNAs. *BMC Genomics* 10:620

38. Lin J-S, Lin C-C, Lin H-H, Chen Y-C, Jeng S-T. (2012) MicroR828 regulates lignin and H_2O_2 accumulation in sweet potato on wounding. *New Phytol* 196:427-440
39. Zhai J, Jeong D-H, De Paoli E, Park S, Rosen BD, Li Y et al. (2011) MicroRNAs as master regulators of the plant NB-LRR defense gene family via the production of phased, *trans*-acting siRNAs. *Genes Dev* 25:2540-2553
40. Zhang C, Li G, Wang J, Fang J. (2012) Identification of *trans*-acting siRNAs and their regulatory cascades in grapevine. *Bioinformatics* 28:2561-2568
41. Guan X, Pang M, Nah G, Shi X, Ye W, Stelly DM et al. (2014) miR828 and miR858 regulate homoeologous MYB2 gene functions in Arabidopsis trichome and cotton fibre development. *Nat Comm* 5:3050
42. Källman T, Chen J, Gyllenstrand N, Lagercrantz U. (2013) A significant fraction of 21 nt sRNA originates from phased degradation of resistance genes in several perennial species. *Plant Physiol* 162:741-754
43. Xia R, Xu J, Arikit S, Meyers BC. (2015) Extensive families of miRNAs and PHAS loci in Norway spruce demonstrate the origins of complex phasiRNA networks in seed plants. *Mol Biol Evol* 32:2905-2918
44. Pantaleo V, Szittya G, Moxon S, Miozzi L, Moulton V, Dalmay T et al. (2010) Identification of grapevine microRNAs and their targets using high-throughput sequencing and degradome analysis. *Plant J* 62:960-976
45. Chiang C-P, Chien P-S, Leong SJ, Chiou T-J. (2018) Sensing and signaling of phosphate starvation: From local to long distance. *Plant Cell Physiol* 59:1714-1722
46. Wang Y, Itaya A, Zhong X, Wu Y, Zhang J, van der Knaap E et al. (2011) Function and evolution of a microRNA that regulates a Ca^{2+}-ATPase and triggers the formation of phased small interfering RNAs in tomato reproductive growth. *Plant Cell* 23:3185-3203
47. Frohnmeyer H, Loyall L, Blatt MR, Grabov A. (1999) Millisecond UV-B irradiation evokes prolonged elevation of cytosolic-free Ca^{2+} and stimulates gene expression in transgenic parsley cell cultures. *Plant J* 20:109-117
48. Lin W-Y, Lin Y-Y, Chiang S-F, Syu C, Hsieh L-C, Chiou T-J. (2018) Evolution of microRNA827 targeting in the plant kingdom. *New Phytol* 217:1712-1725
49. Hackenberg M, Shi B-J, Gustafson P, Langridge P. (2013) Characterization of phosphorus-regulated miR399 and miR827 and their isomirs in barley under phosphorus-sufficient and phosphorus-deficient conditions. *BMC Plant Biol* 13:214
50. Zhang J-P, Yu Y, Feng Y-Z, Zhou Y-F, Zhang F, Yang Y-W et al. (2017) miR408 regulates grain yield and photosynthesis via a phytocyanin protein. *Plant Physiol* 175:1175-1185
51. Bai Q, Wang X, Chen X, Shi G, Liu Z, Guo C et al. (2018) Wheat miRNA tae-miR408 acts as an essential mediator in plant tolerance to P_i deprivation and salt stress via modulating stress-associated physiological processes. *Front Plant Sci* 9:499
52. Zhang F, Zhang Y-C, Zhang J-P, Yu Y, Zhou Y-F, Feng Y-Z et al. (2018) Rice *UCL8*, a plantacyanin gene targeted by miR408, regulates fertility by controlling pollen tube germination and growth. *Rice* 11:60
53. Jhu M-Y, King Y-C, Li Y-C, Kuo Y-W, Jeng S-T, Lin J-S. (2018) MicroR408 regulates defense response upon wounding in sweet potato. *J Exp Bot* 70:469-483
54. Sun M, Yang J, Cai X, Shen Y, Cui N, Zhu Y et al. (2018) The opposite roles of os-miR408 in cold and drought stress responses in *Oryza sativa*. *Mol Breeding* 38:120
55. Zhang W, Gao S, Zhou X, Chellappan P, Chen Z, Zhou X et al. (2011) Bacteria-responsive microRNAs regulate plant innate immunity by modulating plant hormone networks. *Plant Mol Biol* 75:93-105
56. Lu Y-T, Li M-Y, Cheng K-T, Tan CM, Su L-W, Lin W-Y et al. (2014) Transgenic plants that express the phytoplasma effector SAP11 show altered phosphate starvation and defense responses. *Plant Physiol* 164:1456-1469
57. Liu T-Y, Aung K, Tseng C-Y, Chang T-Y, Chen Y-S, Chiou T-J. (2011) Vacuolar Ca^{2+}/H^+ transport activity is required for systemic phosphate homeostasis involving shoot-to-root signaling in Arabidopsis. *Plant Physiol* 156:1176-1189
58. Choi H-K, Iandolino A, da Silva FG, Cook DR. (2013) Water deficit modulates the response of *Vitis vinifera* to the Pierce's disease pathogen *Xylella fastidiosa*. *Mol Plant-Microbe Interact* 26:643-657
59. Rogers EE. (2012) Evaluation of *Arabidopsis thaliana* as a model host for *Xylella fastidiosa*. *Mol Plant-Microbe Interact* 25:747-754
60. Fei Q, Xia R, Meyers BC. (2013) Phased, secondary, small interfering RNAs in posttranscriptional regulatory networks. *Plant Cell* 25:2400-2415

61. Xia R, Meyers BC, Liu Z, Beers EP, Ye S, Liu Z. (2013) MicroRNA superfamilies descended from miR390 and their roles in secondary small interfering RNA biogenesis in Eudicots. *Plant Cell* 25:1555-1572
62. Axtell MJ, Jan C, Rajagopalan R, Bartel DP. (2006) A two-hit trigger for siRNA biogenesis in plants. *Cell* 127:565-577
63. Montgomery TA, Howell MD, Cuperus JT, Li DW, Hansen JE, Alexander AL et al. (2008) Specificity of ARGONAUTE7-miR390 interaction and dual functionality in *TAS3 trans*-acting siRNA formation. *Cell* 133:128-141
64. Deng P, Muhammad S, Cao M, Wu L. (2018) Biogenesis and regulatory hierarchy of phased small interfering RNAs in plants. *Plant Biotech J* 16:965-975
65. Guo QL, Qu XF, Jin WB. (2015) PhaseTank: genome-wide computational identification of phasiRNAs and their regulatory cascades. *Bioinformatics* 31:284-286
66. Brilli M, Asquini E, Moser M, Bianchedi PL, Perazzolli M, Si-Ammour A. (2018) A multi-omics study of the grapevine-downy mildew (*Plasmopara viticola*) pathosystem unveils a complex protein coding- and noncoding-based arms race during infection. *Sci Rep* 8:757
67. Zhao MX, Cai CM, Zhai JX, Lin F, Li LH, Shreve J et al. (2015) Coordination of microRNAs, phasiRNAs, and NB-LRR genes in response to a plant pathogen: insights from analyses of a set of soybean *Rps* gene near-isogenic lines. *Plant Genome* 8:doi: 10.3835/plantgenome2014.3809.0044
68. Di Gaspero G, Cipriani G, Adam-Blondon AF, Testolin R. (2007) Linkage maps of grapevine displaying the chromosomal locations of 420 microsatellite markers and 82 markers for R-gene candidates. *Theor Appl Genet* 114:1249-1263
69. Sun XM, Fan GT, Su LY, Wang WJ, Liang ZC, Li SH et al. (2015) Identification of cold-inducible microRNAs in grapevine. *Front Plant Sci* 6:595
70. Plessis A, Cournol R, Effroy D, Silva Pérez V, Botran L, Kraepiel Y et al. (2011) New ABA-hypersensitive Arabidopsis mutants are affected in loci mediating responses to water deficit and *Dickeya dadantii* infection. *PLoS ONE* 6:e20243
71. Fahlgren N, Carrington JC. (2010)miRNA target prediction in plants. In: *Plant microRNAs*. Edited by Meyers BC, Green PJ, vol. 592: Humana Press: 51-57.
72. Wang H, Chung PJ, Liu J, Jang I-C, Kean MJ, Xu J et al. (2014) Genome-wide identification of long noncoding natural antisense transcripts and their responses to light in Arabidopsis. *Genome Res* 24:444-453
73. Yadav V, Molina I, Ranathunge K, Castillo IQ, Rothstein SJ, Reed JW. (2014) ABCG transporters are required for suberin and pollen wall extracellular barriers in *Arabidopsis*. *Plant Cell* 26:3569-3588
74. Barberon M, Vermeer Joop Engelbertus M, De Bellis D, Wang P, Naseer S, Andersen Tonni G et al. (2016) Adaptation of root function by nutrient-induced plasticity of endodermal differentiation. *Cell* 164:447-459
75. Thieme CJ, Rojas-Triana M, Stecyk E, Schudoma C, Zhang W, Yang L et al. (2015) Endogenous Arabidopsis messenger RNAs transported to distant tissues. *Nat Plants* 1:15025
76. Lin SI, Chiang SF, Lin WY, Chen JW, Tseng CY, Wu PC et al. (2008) Regulatory network of microRNA399 and PHO2 by systemic signaling. *Plant Physiol* 147:732-746
77. Lin S-I, Santi C, Jobet E, Lacut E, El Kholti N, Karlowski WM et al. (2010) Complex regulation of two target genes encoding SPX-MFS proteins by rice miR827 in response to phosphate starvation. *Plant Cell Physiol* 51:2119-2131
78. Zhao MX, Meyers BC, Cai CM, Xu W, Ma JX. (2015) Evolutionary patterns and coevolutionary consequences of MIRNA genes and microRNA targets triggered by multiple mechanisms of genomic duplications in soybean. *Plant Cell* 27:546-562
79. Wallis CM, Chen J. (2012) Grapevine phenolic compounds in xylem sap and tissues are significantly altered during infection by *Xylella fastidiosa*. *Phytopathology* 102:816-826
80. Wallis CM, Wallingford AK, Chen J. (2013) Grapevine rootstock effects on scion sap phenolic levels, resistance to *Xylella fastidiosa* infection, and progression of Pierce's disease. *Front Plant Sci* 4:502
81. Langmead B, Trapnell C, Pop M, Salzberg S. (2009) Ultrafast and memory-efficient alignment of short DNA sequences to the human genome. *Genome Biol* 10:R25
82. Wallis CM, Wallingford AK, Chen J. (2013) Effects of cultivar, phenology, and *Xylella fastidiosa* infection on grapevine xylem sap and tissue phenolic content. *Physiol Mol Plant Pathol* 84:28-35
83. Velten J, Cakir C, Cazzonelli CI. (2010) A spontaneous dominant-negative mutation within a 35S::*AtMYB90* transgene inhibits flower pigment production in tobacco. *PLoS ONE* 5:e9917

84. Lang Q, Jin C, Lai L, Feng J, Chen S, Chen J. (2011) Tobacco microRNAs prediction and their expression infected with *Cucumber mosaic virus* and *Potato virus X*. *Mol Biol Rep* 38:1523-1531
85. Velten J, Cakir C, Youn E, Chen J, Cazzonelli CI. (2012) Transgene silencing and transgene-derived siRNA production in tobacco plants homozygous for an introduced *AtMYB90* construct. *PLoS ONE* 7:e30141